Sandia National Laboratories

Exceptional service in the national interest

ATOMISTIC MODELING OF MATERIALS FOR FUSION ENERGY USING MACHINE LEARNED INTERATOMIC POTENTIALS

M.A. Cusentino[1]

[1]Sandia National Laboratories

LAMMPS Workshop 2025

August 14, 2025

Sandia National Laboratories is a multimission laboratory managed and operated by National Technology and Engineering Solutions of Sandia, LLC, a wholly owned subsidiary of Honeywell International Inc., for the U.S. Department of Energy's National Nuclear Security Administration under contract DE-NA0003525

SAND2025-03199C

Thanks To All Collaborators!

Sandia National Laboratories

James Goff

Megan McCarthy

Ember Salas

Aidan Thompson

Mitch Wood

University of New Mexico

Shane Evans

Eric Lang

Stony Brook University

Yusheng Jin

Anas Manzoor

Spencer Thomas

Jason Trelewicz

University of Tennessee Knoxville

Katie Karl

University of California San Diego

Matt Baldwin

Materials For Fusion Energy

- Difficult to develop materials to handle extreme conditions within tokamak
- Large heat loads of 10-20 MW/m^3
- High particles fluxes of ~10^{24} m^{-2}s^{-1} of mixed ion species (H/He/Be/N etc.)

W-Be Intermetallics

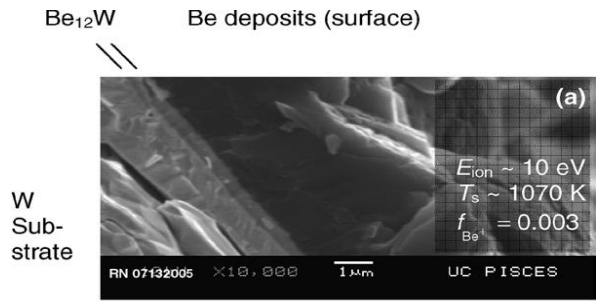

Baldwin, et. al. J. Nucl. Mater. 363-365 (2007) 1179-1183

Helium Fuzz Growth

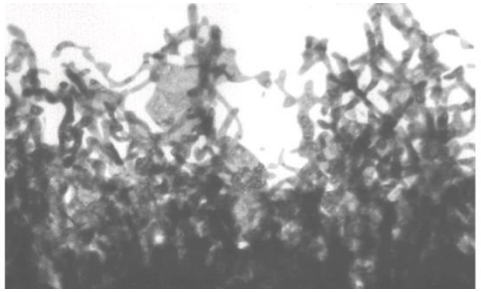

Kajita, et al. J. Nucl. Mater, 418, (2011) 152-158

Hydrogen Blisters

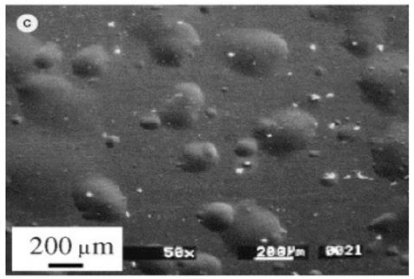

Ye, et al. J. Nucl. Mater. 313-316, 72-76 (2003)

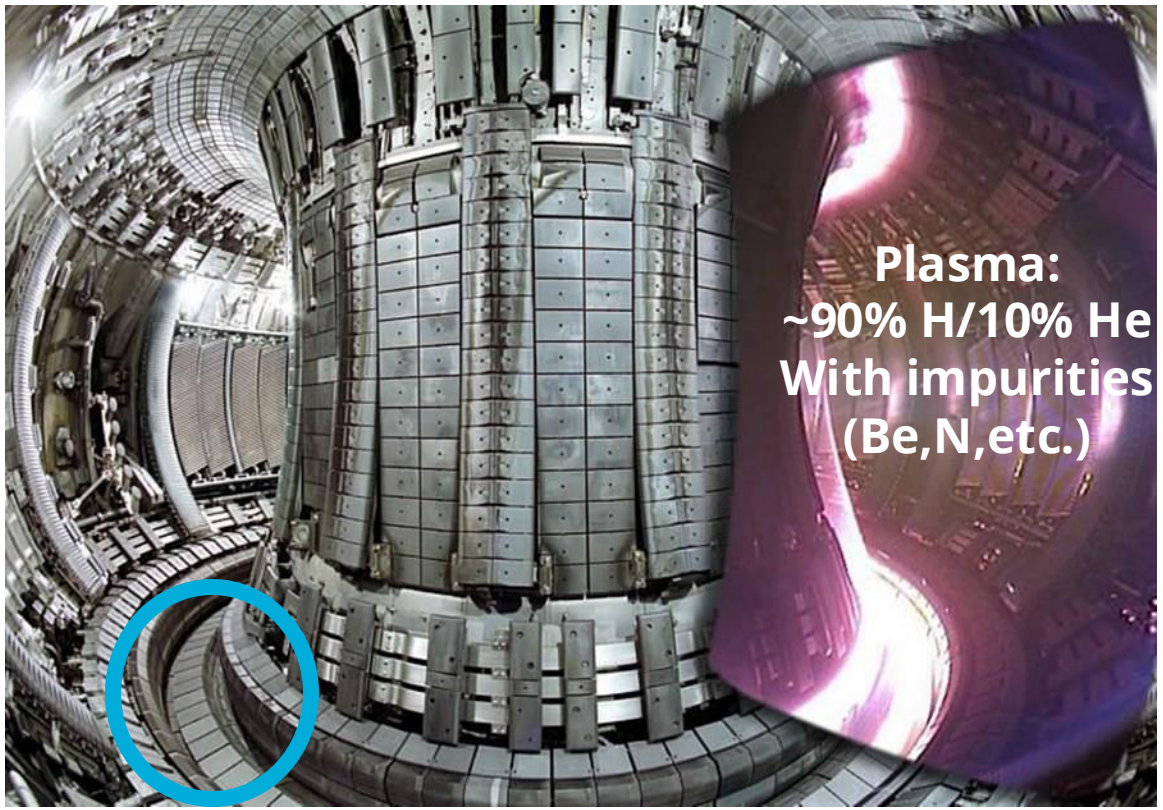

Tungsten Divertor

iter.org

Materials For Fusion Energy

- Difficult to develop materials to handle extreme conditions within tokamak
- Large heat loads of 10-20 MW/m^3
- High particles fluxes of ~10^{24} m^{-2}s^{-1} of mixed ion species (H/He/Be/N etc.)

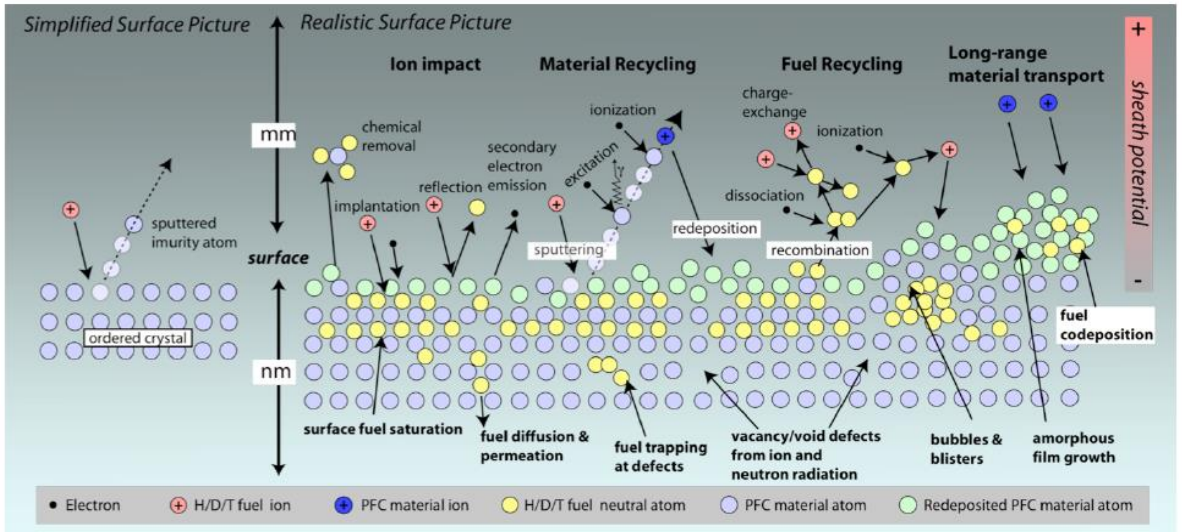

Wirth, et al. MRS Bulletin 36 (2011) 216-222

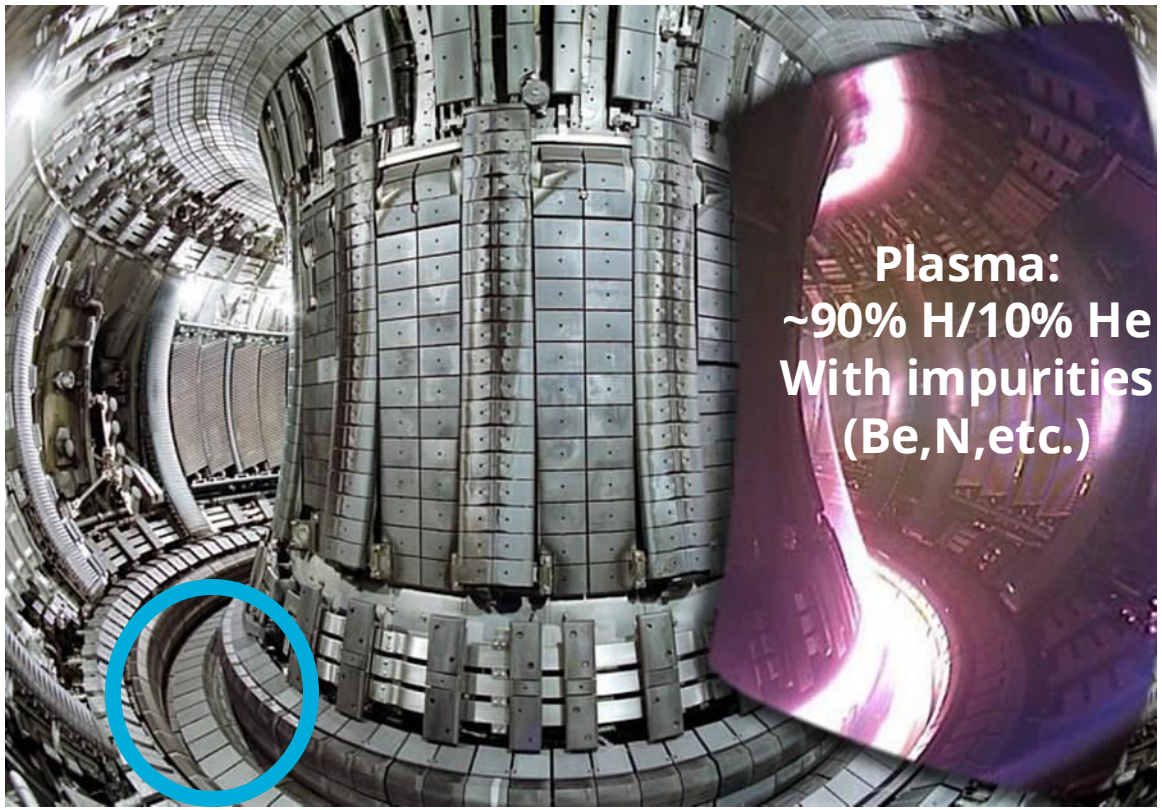

Tungsten Divertor

iter.org

- Many complex processes that occur at the plasma/material interface that can lead to material degradation

Why Do We Need ML-IAPs?

We want to model very complex physics and chemistry at the plasma-material interface.
How do we do this?

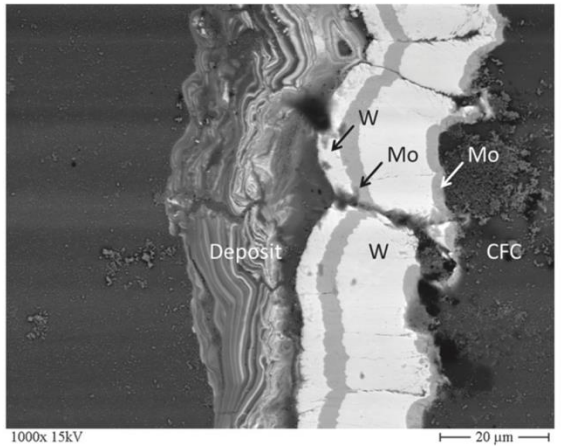

M Mayer *et al* 2016 *Phys. Scr.* **2016** 014051

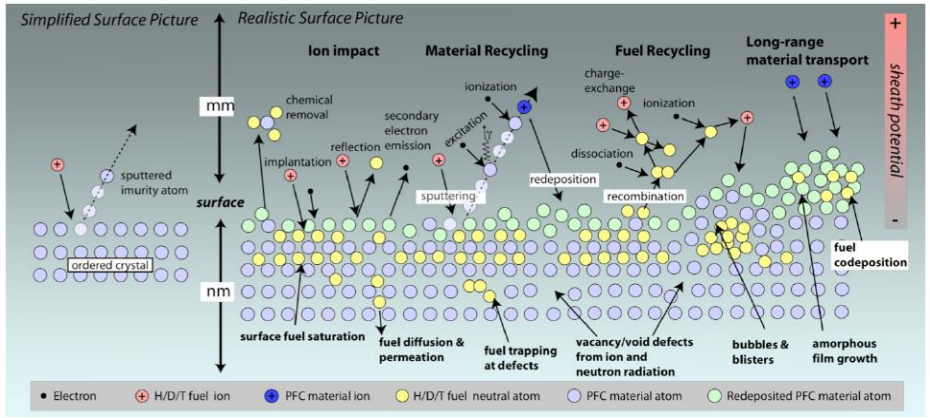

Wirth, et al. MRS Bulletin 36

Electronic Structure Methods

- Highly accurate
- Can model a lot of relevant physics
- Very expensive, $O(N^3)$ scaling, ~100 atoms

Classical Potentials

- Lots of functional forms that are good for many different materials
- Scales well
- Accuracy highly dependent on potential and application
- Functional form limits type of physics that can be modeled

Machine Learned Interatomic Potentials

- Trained to electronic structure data for increased accuracy
- Flexible, not limited by inherent physics of model
- Quantum accuracy but MD scalability
- Need good training data for accurate model

What Makes A Machine Learned Interatomic Potential?

Training Data

- Generated using quantum methods
- Can include:
  - Energies
  - Forces
  - Stresses
- Variety of atomic configurations
  - Bulk structures, liquids, surfaces, defects, etc.

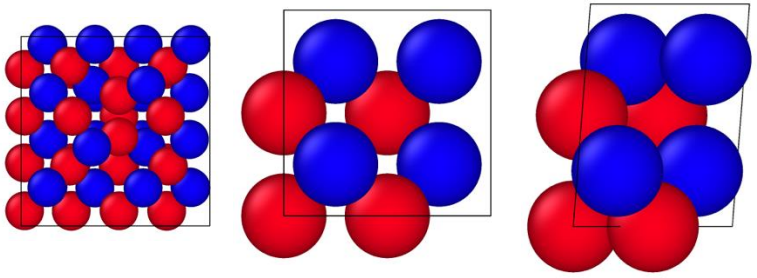

Descriptor

- Describes the local atomic environment
- Requirements
  - Rotation/Translation/. Permutation invariant
  - Equivariant forces
  - Smooth differentiable
  - Extensible
- Some Examples
  - Bispectrum, SOAP, ACE, Moment Tensors, etc.

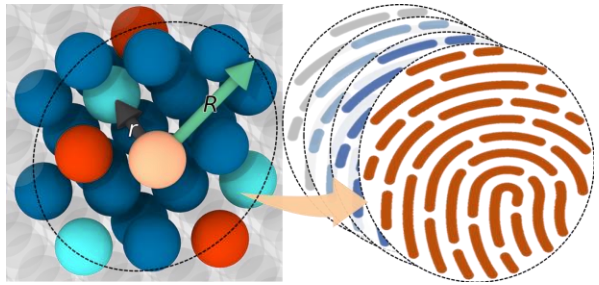

Regression Method

- Linear regression
- Kernel ridge regression
- Gaussian process
- Non-linear optimization
- Neural Networks

ACE

- Energies, forces, and stresses from DFT
- Atomic Cluster Expansion descriptors
- Linear regression

ACE Definition and FitSNAP Work Flow

Model Form

- Energy of atom i expressed as a basis expansion over N-body ACE descriptors

$$E = \sum B^{N=1} + \sum B^{N=2} + \sum B^{N=3} + \cdots$$

The ACE descriptors are generalizable

Regression Method

- β vector fully describes a ACE potential
- Decouples MD speed from training set size

$$\min(||\mathbf{w} \cdot D\boldsymbol{\beta} - T||^2 - \gamma_n \, ||\boldsymbol{\beta}||^n)$$

Weights — Set of Descriptors — DFT Training

ACE Development Workflow

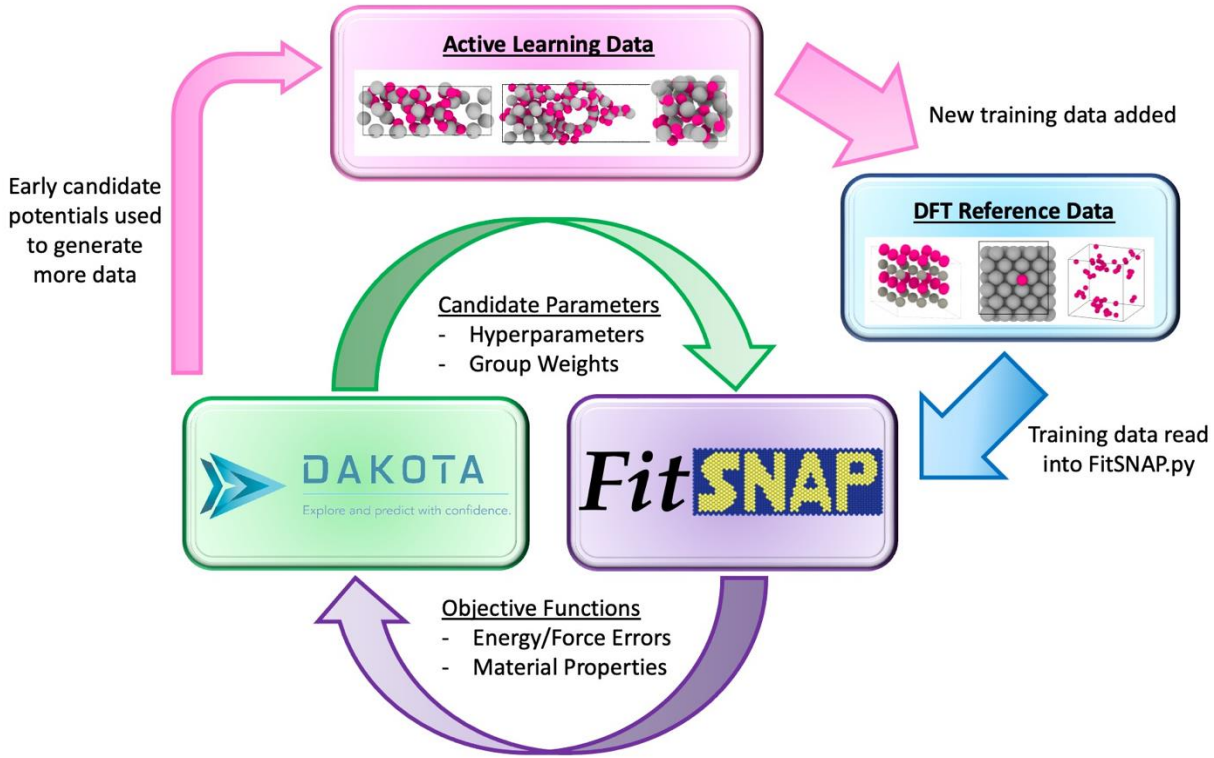

Code available: https://github.com/FitSNAP/FitSNAP

Rohskopf et al., (2023). FitSNAP: Atomistic machine learning with LAMMPS. Journal of Open Source Software, 8(84), 5118

Fusion ML-IAPs Developed

SNAP W-Be

Simulated initial formation of experimentally observed W-Be intermetallics

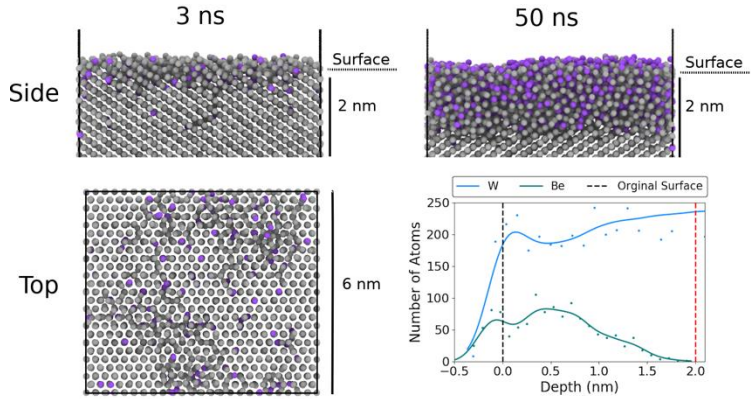

Cusentino, et al. Nucl. Fusion, 61 (2021) 046049

SNAP W-Be-He

W-Be intermetallics inhibited He bubble nucleation and growth

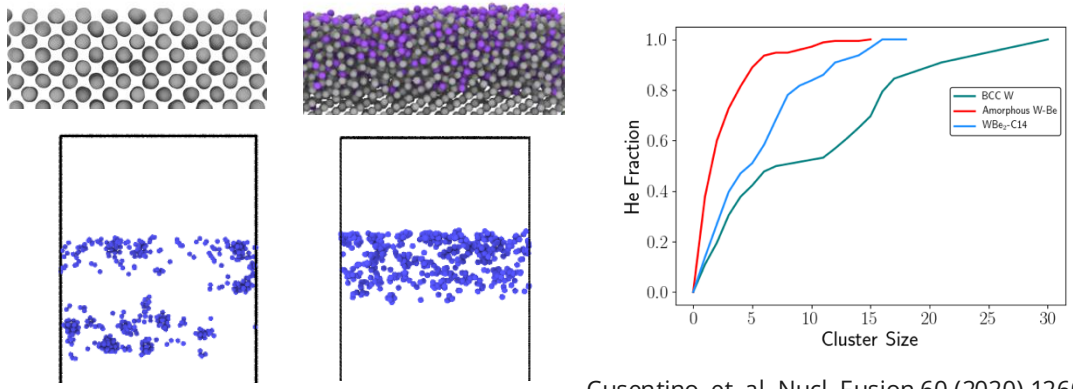

Cusentino, et. al. Nucl. Fusion 60 (2020) 126018

SNAP W-H

Studied formation of H platelets at high H fluences

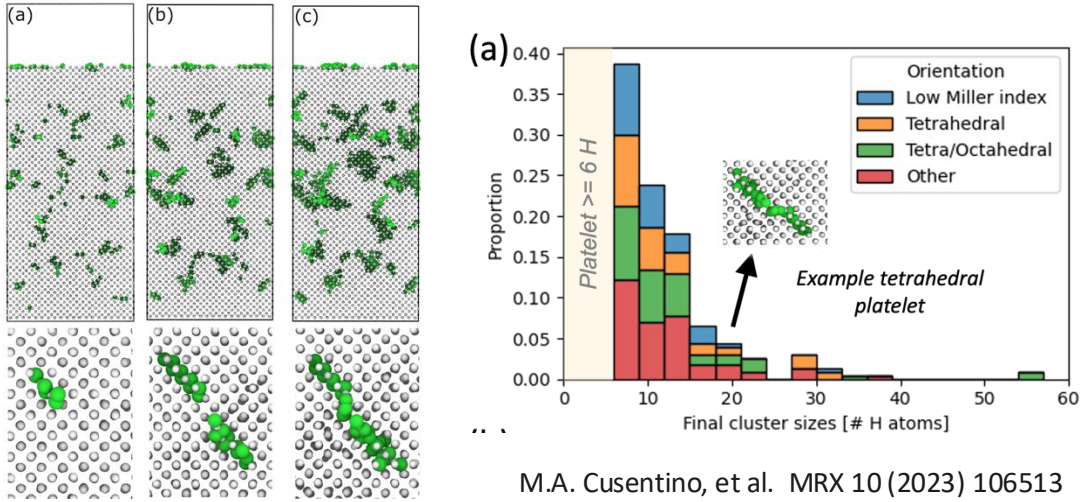

M.A. Cusentino, et al. MRX 10 (2023) 106513

SNAP W-ZrC

Modeled impact of temperature on strength of W-ZrC

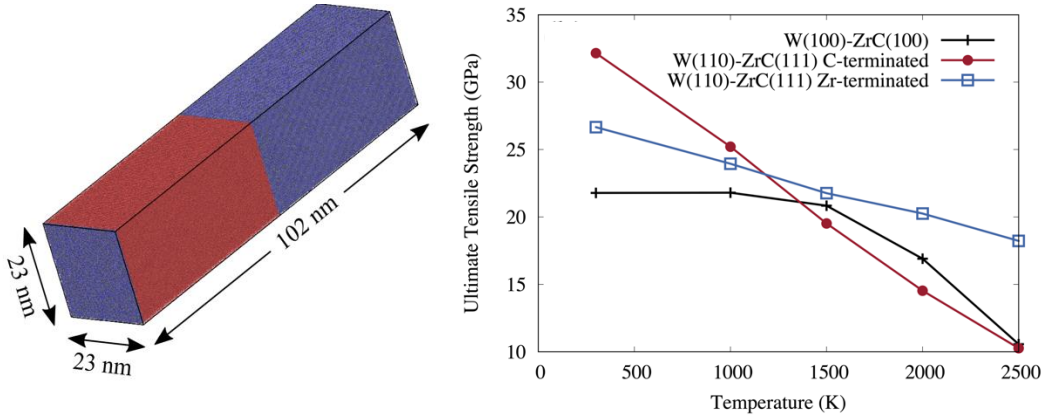

Sikorski, et al. *J. Chem. Phys.* 158 (2023) 11

Role Of Transmutation Products On First Wall Materials (SciDAC-5)

- First wall materials will be subject to extreme environments including neutron irradiation which will alter material chemistry through transmutation
- How will this impact:
  - Thermomechanical properties
  - Defect properties
- Lack of fusion prototypic neutron source emphasizes need for multiscale models of the effect of transmutation products on first-wall materials
- Molecular dynamics will play a key role but lack of accurate interatomic potentials for these material systems:
  - W-Re-Os
  - Fe-Cr-Mn-W
  - SiC-Mg

First Wall Design Reference

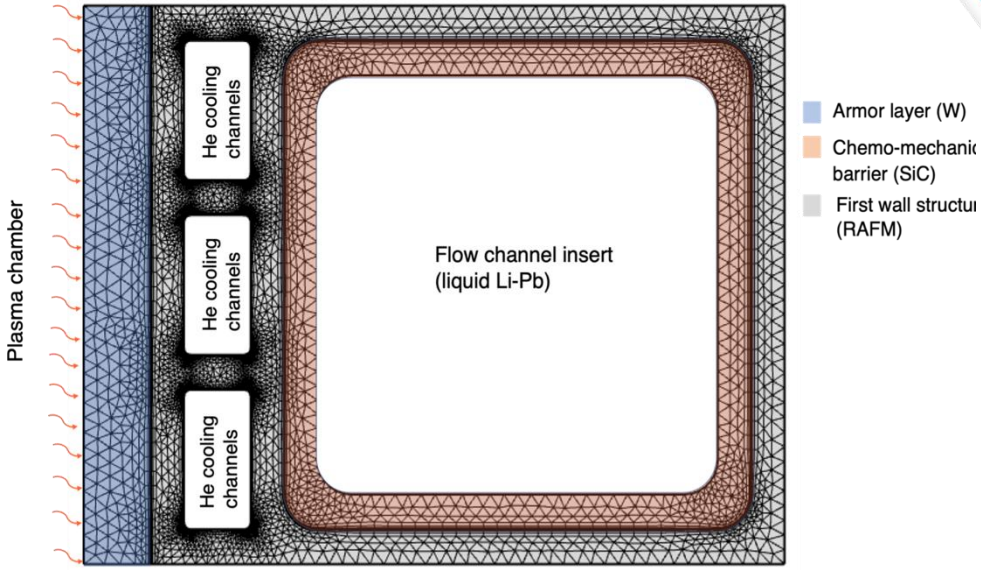

Transmutation Products in W

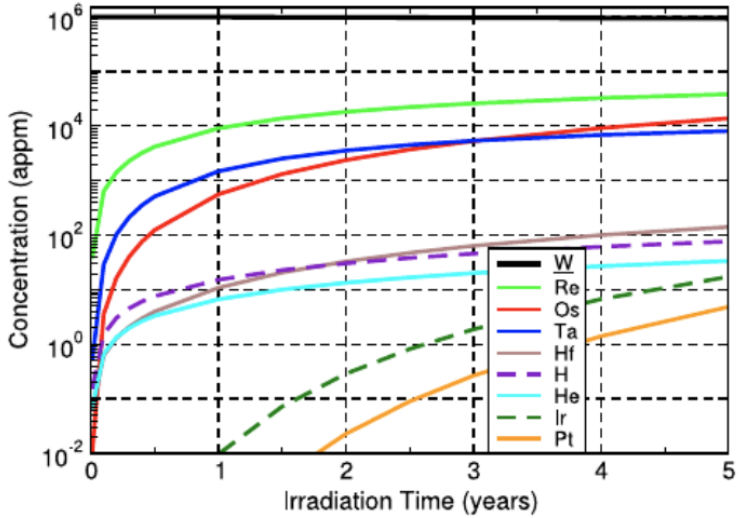

M.R. Gilbert and J.-Ch Sublet, Nucl. Fusion 51 (2011) 043005 (13pp)

Goals for W-Re-Os ML-IAP Development

- Re and Os are the main transmutation product in W
- Re is shown to cluster and form precipitates in W
  - Interested in studying this behavior but current potentials predict incorrect Re-Re binding energies in W compared to DFT
  - Re should only cluster when vacancies are present
- Focus fitting of potential on accurate defect properties to study the effect of vacancies on Re clustering in W with accurate IAP
- Interested in studying thermomechanical properties as well

Re-Re and Os-Os Binding Energies in W

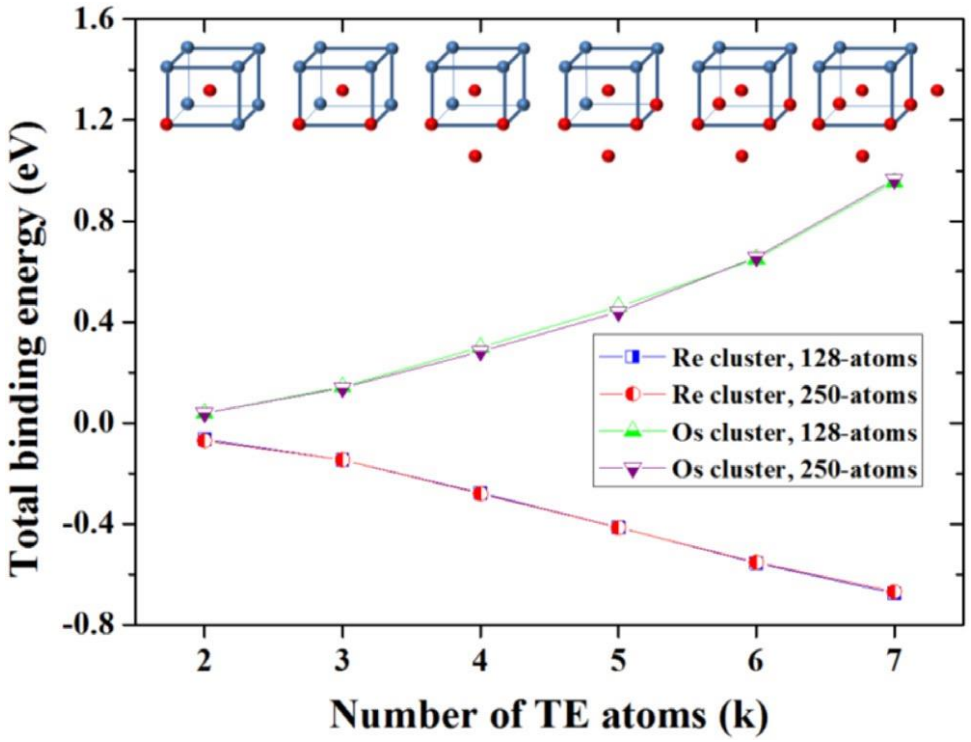

Yu-Hao Li et al 2017 Nucl. Fusion 57 046006

W-Re Training Set

Grey: W **Blue:** Re

Deformed Unit Cells

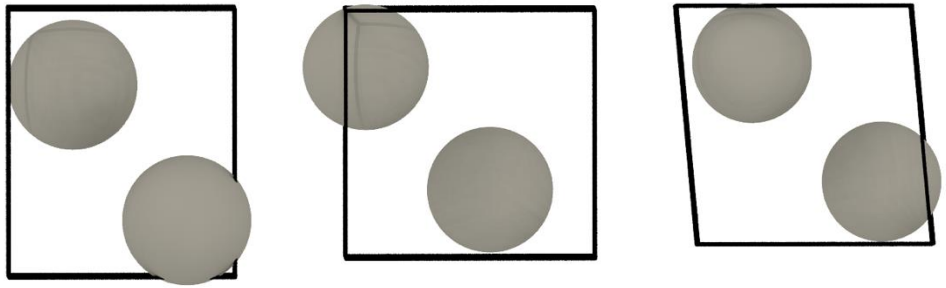

Elastically strained, sheared, and compressed/expanded unit cells

W-Re Intermetallics

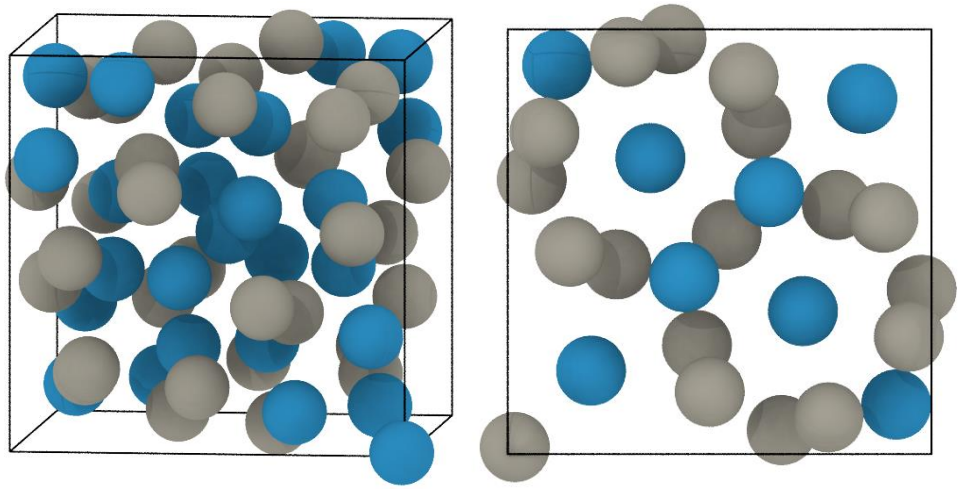

Chi and Sigma phases

N_E : 13,345

N_F : 793,689

Defect Configurations

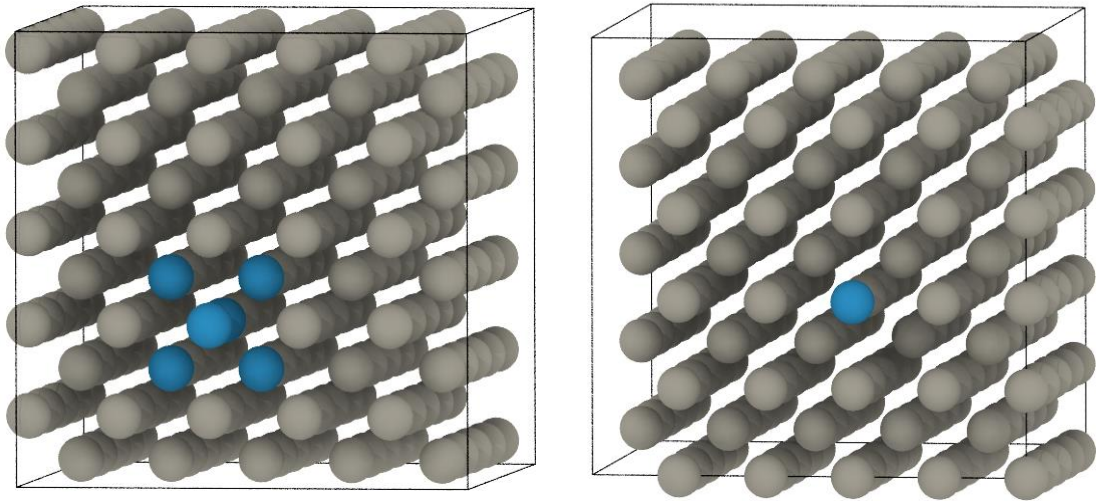

Point Defects, Re-Re, and Re-V configurations

DFT-MD

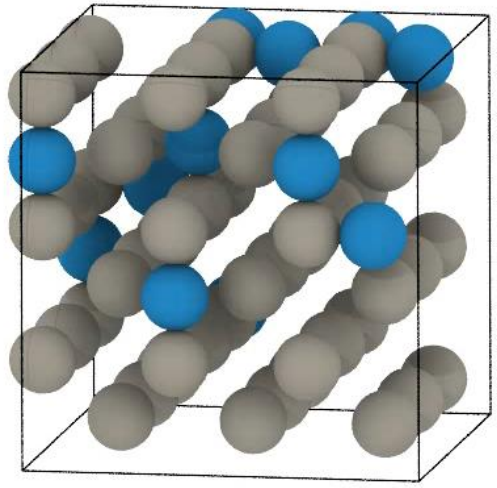

Pure W, pure Re, and mixed W-Re at 4000 K

Pure Phases

Deformed unit cells, DFT-MD, Surfaces, Dimers, Defects

Alloys

Deformed unit cells, DFT-MD, Defects Interactions, Intermetallics

Fitting W-Re ACE ML-IAP

Parameters to optimize:

- Radial cutoff (r_{cut}) for each element and cross-term
- Inner cutoff ($r_{cutinner}$) for each element and cross-term (related to ZBL switching function)
- λ for each element and cross-term, determines emphasis of short range interactions
- Energy and force groupweights in linear regression

Optimize Single Element Potentials then Freeze Parameters and Combine

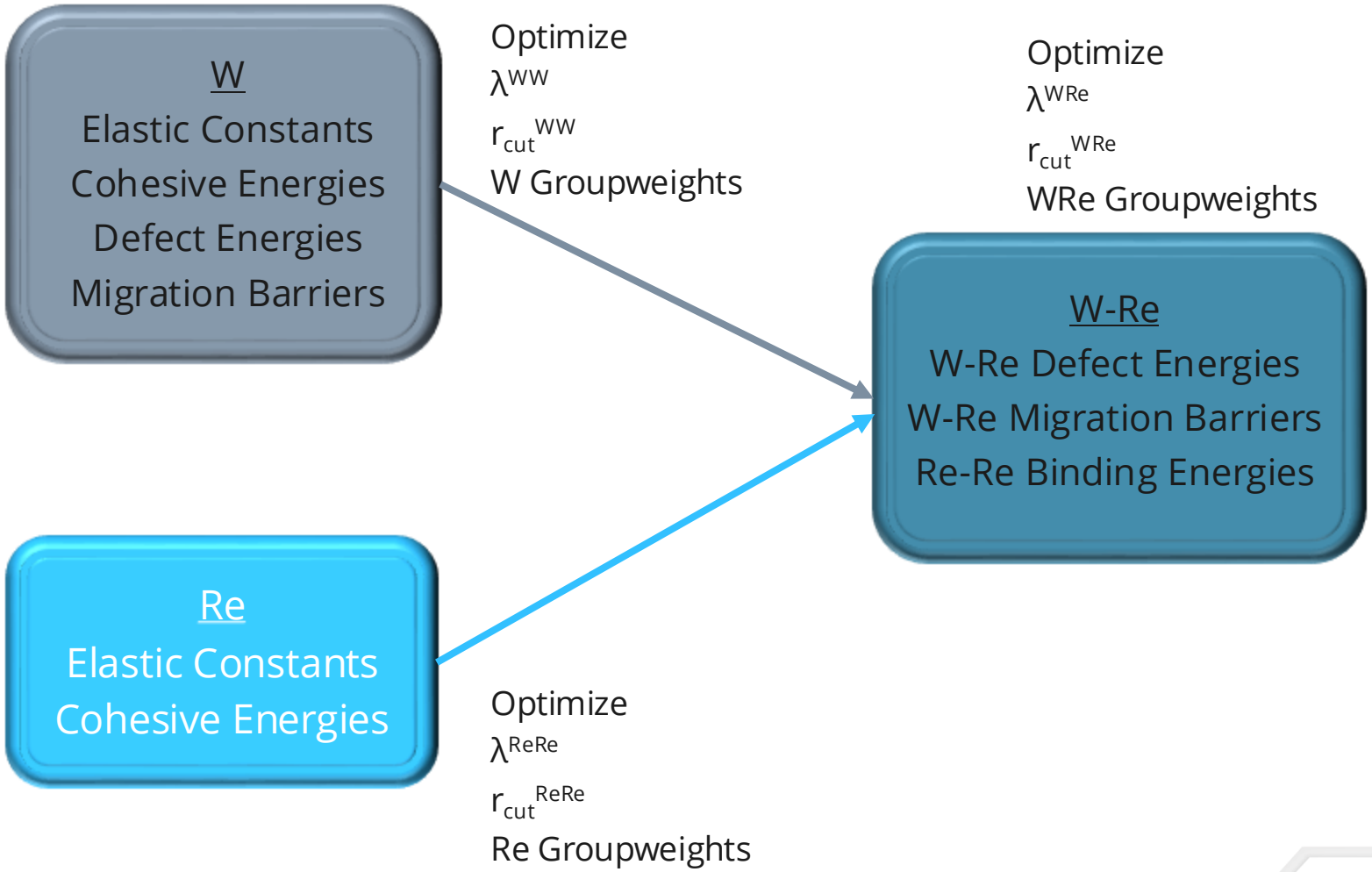

Fitting W-Re ACE ML-IAP

Parameters to optimize:

- Radial cutoff (r_{cut}) for each element and cross-term
- Inner cutoff ($r_{cutinner}$) for each element and cross-term (related to ZBL switching function)
- λ for each element and cross-term, determines emphasis of short range interactions
- Energy and force groupweights in linear regression

Optimize Single Element Potentials then Freeze Parameters and Combine

Elastic Constants	W ACE (DFT)
C11 (GPa)	486 (517)
C12 (GPa)	199 (198)
C13 (GPa)	-
C33 (GPa)	-
C44 (GPa)	128 (142)

Elastic Constants	Re ACE (DFT)
C11 (GPa)	614 (614)
C12 (GPa)	292 (285)
C13 (GPa)	164 (165)
C33 (GPa)	271 (222)
C44 (GPa)	677 (673)

Optimize
λ^{WW}
r_{cut}^{WW}
W Groupweights

Optimize
λ^{ReRe}
r_{cut}^{ReRe}
Re Groupweights

Optimize
λ^{WRe}
r_{cut}^{WRe}
WRe Groupweights

Elastic Constants	W ACE (DFT)	Re ACE (DFT)
C11 (GPa)	564 (517)	586 (614)
C12 (GPa)	231 (198)	302 (285)
C13 (GPa)	-	128 (165)
C33 (GPa)	-	243 (222)
C44 (GPa)	153 (142)	647 (673)

Initial W-Re Optimization

Elastic Constants	W ACE (DFT)	Re ACE (DFT)
C11 (GPa)	564 (517)	586 (614)
C12 (GPa)	231 (198)	302 (285)
C13 (GPa)	-	128 (165)
C33 (GPa)	-	243 (222)
C44 (GPa)	153 (142)	647 (673)

E_{coh}	W	Re
BCC (eV)	-8.91 (-8.9)	-7.76 (-7.71)
HCP (eV)	-	-8.02 (-8.03)
FCC (eV)	-8.66 (-8.4)	-7.95 (-7.96)
Trigonal (eV)	-	-8.00 (-7.97)

Defect E_f	W ACE (DFT)	Re ACE (DFT)
100 Dumbbell (eV)	-	10.3 (11.4)
110 Dumbbell (eV)	9.61 (10.7)	8.90 (9.4)
111 Dumbbell (eV)	8.67 (10.4)	8.57 (9.3)
Vac/Sub (eV)	3.08 (3.27)	0.17 (0.13)

Migration Barriers

Vac	W SIA	Re
2.29 (1.69)	0.02 (0.003)	0.13 (0.12)

Re-Re Binding Energies

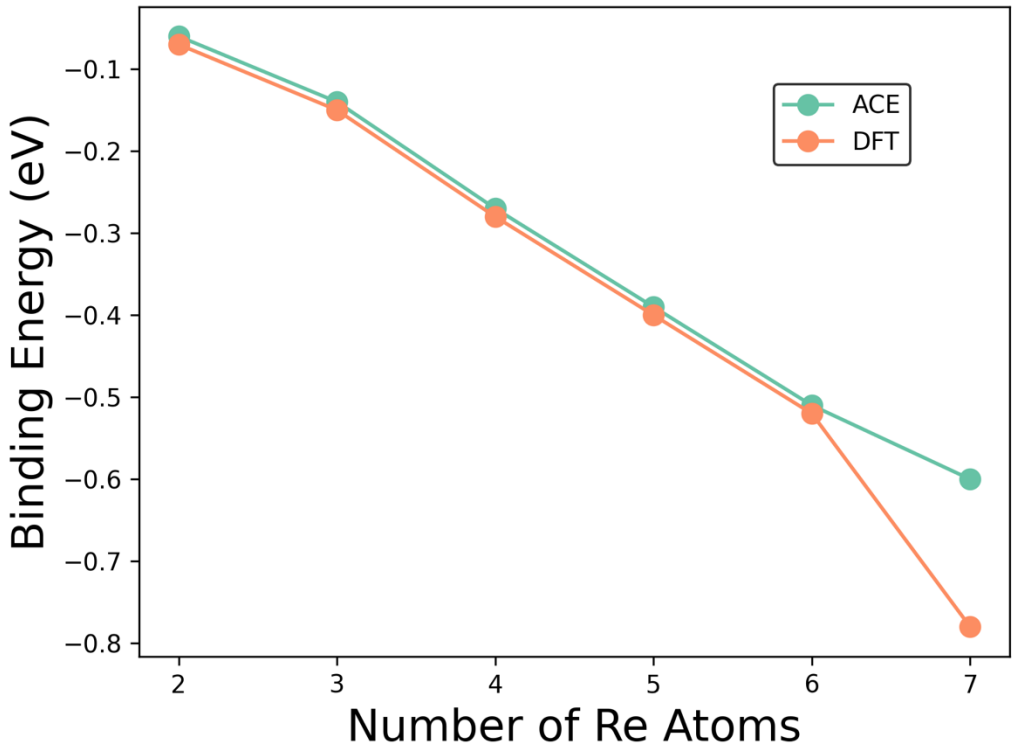

Testing Of Initial W-Re ML-IAP – Issue With Ordered Phase

ACE successfully used for 5 KeV PKA Simulation

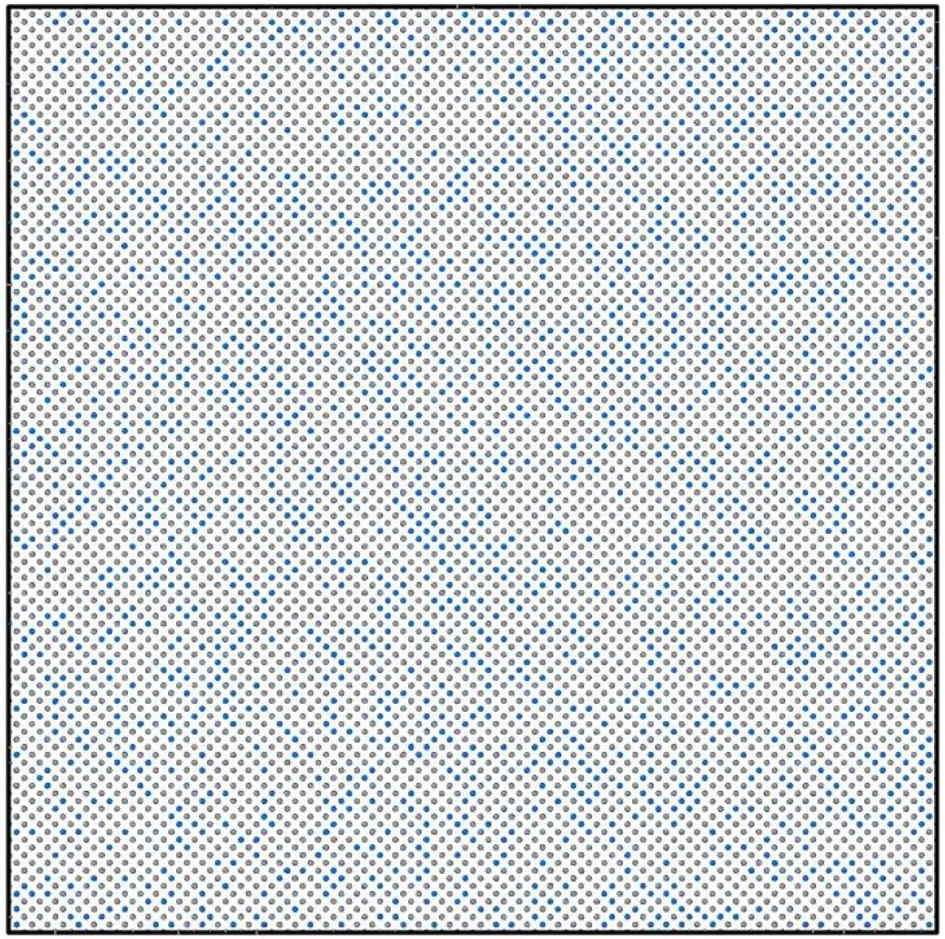

MC-MD Results Indicate Formation of Ordered Phase at Low Temperatures

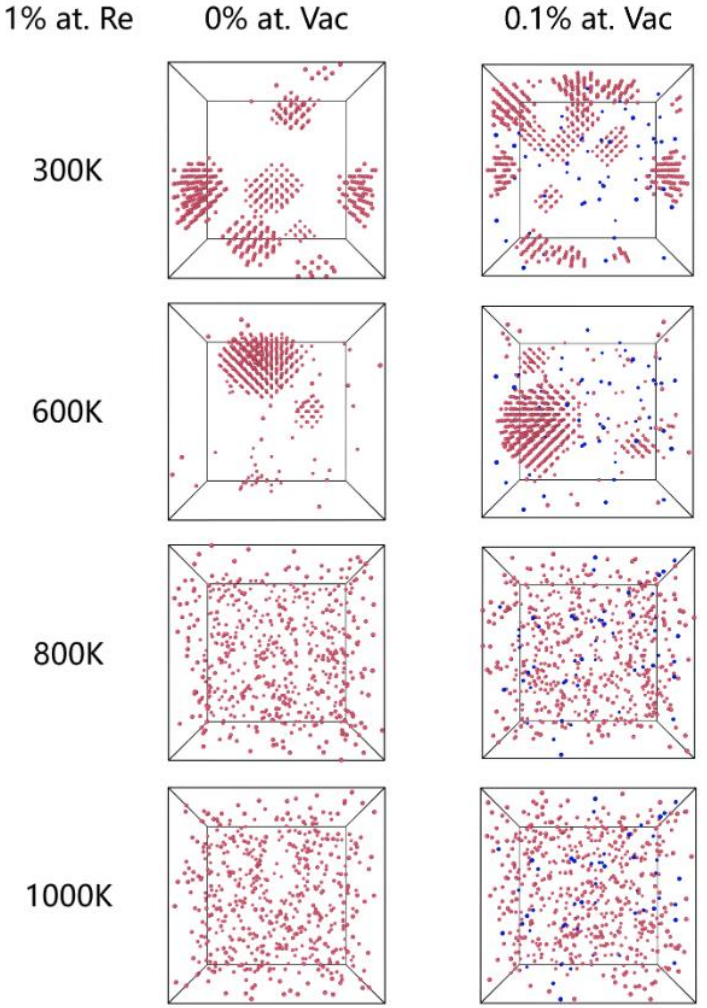

ACE Underpredicts Re-V Binding Energy

Re-V E_B	ACE	DFT
1NN	0.14	0.3
2NN	-0.03	0.25
3NN	-0.08	0.05
4NN	0.03	0.08
5NN	-0.03	0.1

*MC-MD performed by Yusheng Jin and Spencer Thomas (SBU)

Ordered Phase Due to Positive Re-Re Binding Energy

Re-Re 2NN Binding Energy Too High

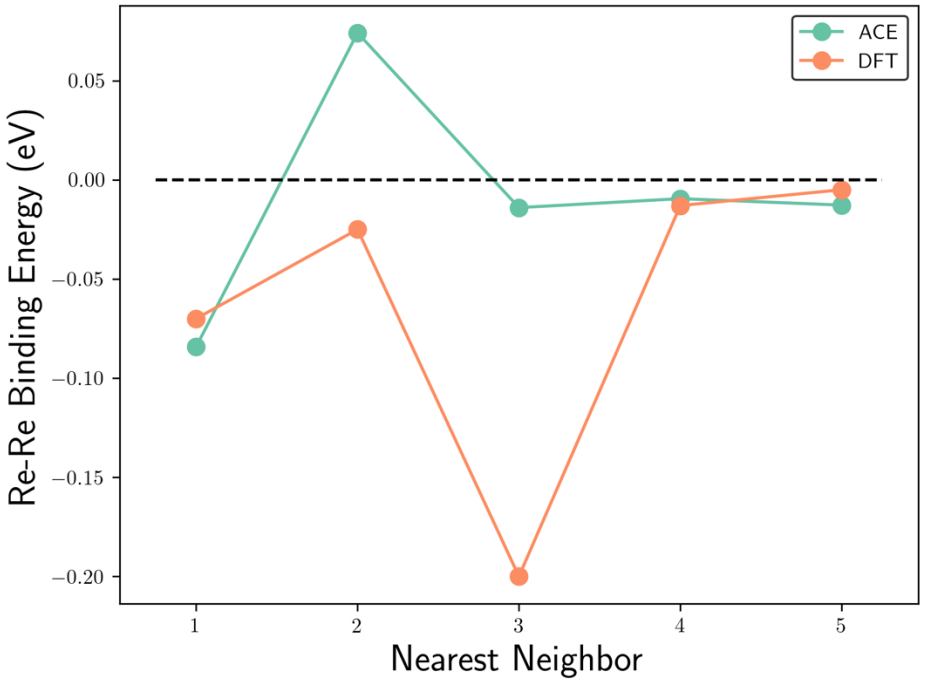

Attractive Re-Re binding energy at 2NN resulting in ordered phase forming

Re-Fit of W-Re ML-IAP

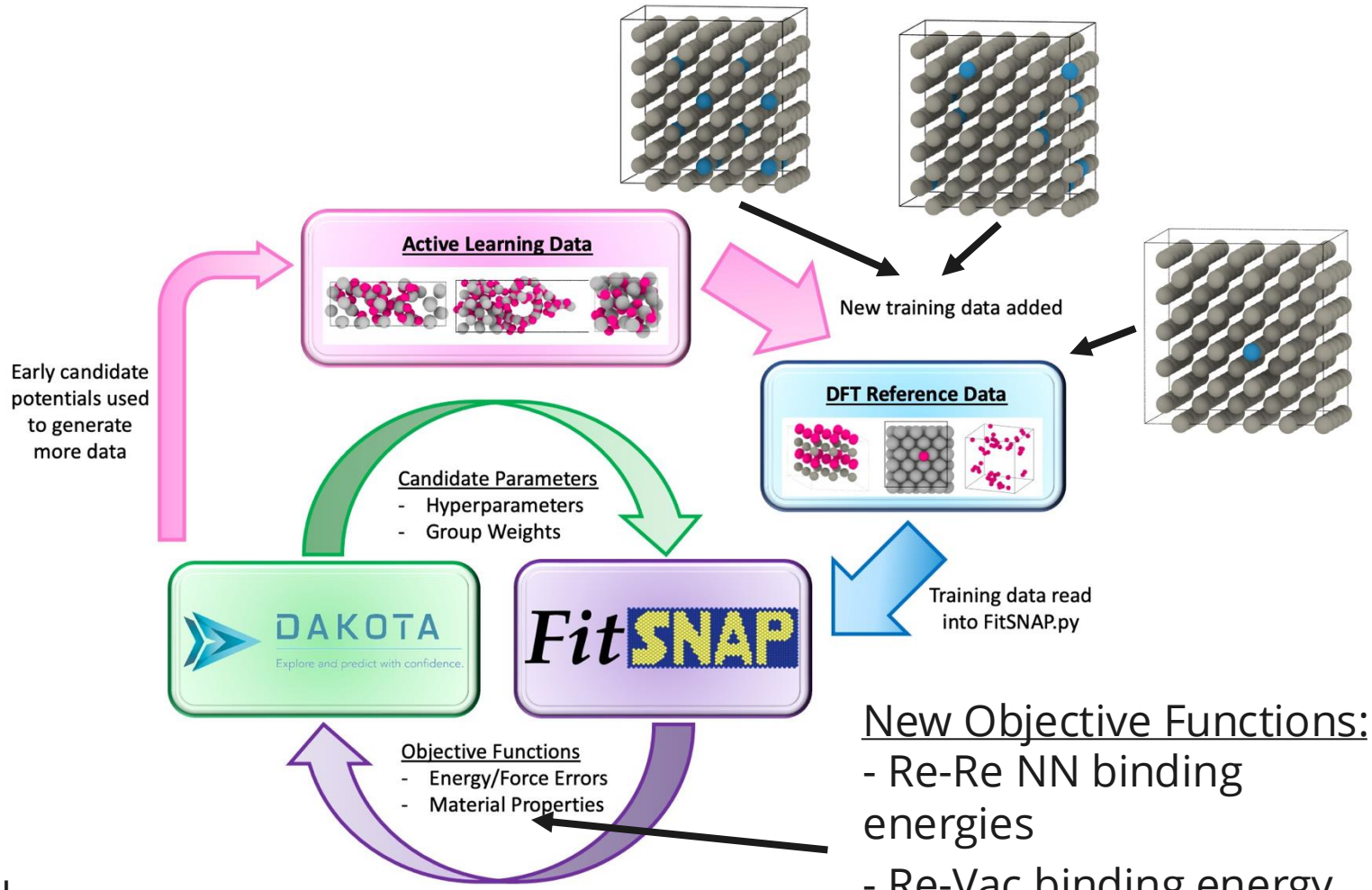

New Objective Functions:
- Re-Re NN binding energies
- Re-Vac binding energy

Refit ACE W-Re ML-IAP

Elastic Constants	W ACE (DFT)	Re ACE (DFT)
C11 (GPa)	360 (517)	635 (614)
C12 (GPa)	240 (198)	298 (285)
C13 (GPa)	-	103 (165)
C33 (GPa)	-	218 (222)
C44 (GPa)	128 (142)	669 (673)

E_{coh}	W	Re
BCC (eV)	-8.9 (-8.9)	-7.79 (-7.71)
HCP (eV)	-	-8.03 (-8.03)
FCC (eV)	-8.8 (-8.4)	-7.94 (-7.96)
Trigonal (eV)	-	-8.00 (-7.97)

Energy error: 0.034 eV/atom

Force error: 0.18 eV/Å-atom

Defect E_f	W ACE (DFT)	Re ACE (DFT)
100 Dumbbell (eV)	-	8.35 (11.4)
110 Dumbbell (eV)	8.92 (10.7)	7.50 (9.4)
111 Dumbbell (eV)	7.76 (10.4)	6.86 (9.3)
Vac/Sub (eV)	2.90 (3.27)	-0.18 (0.13)

Migration Barriers

Vac	W SIA	Re
2.29 (1.69)	0.001 (0.003)	0.12 (0.12)

Re NN Binding

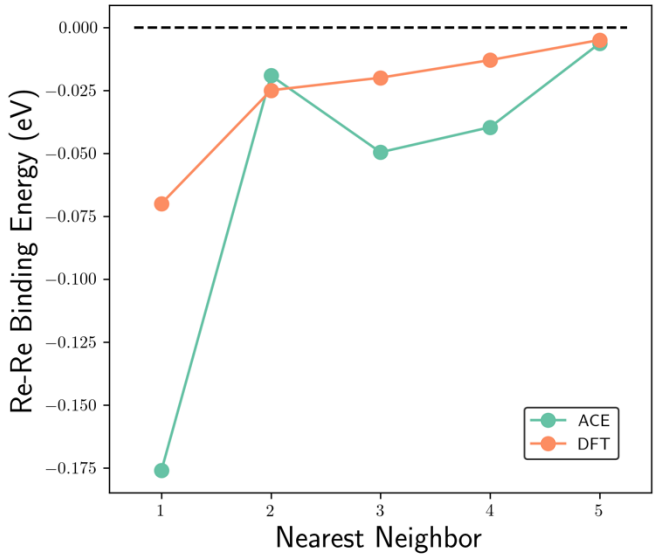

Re-V Binding Energies

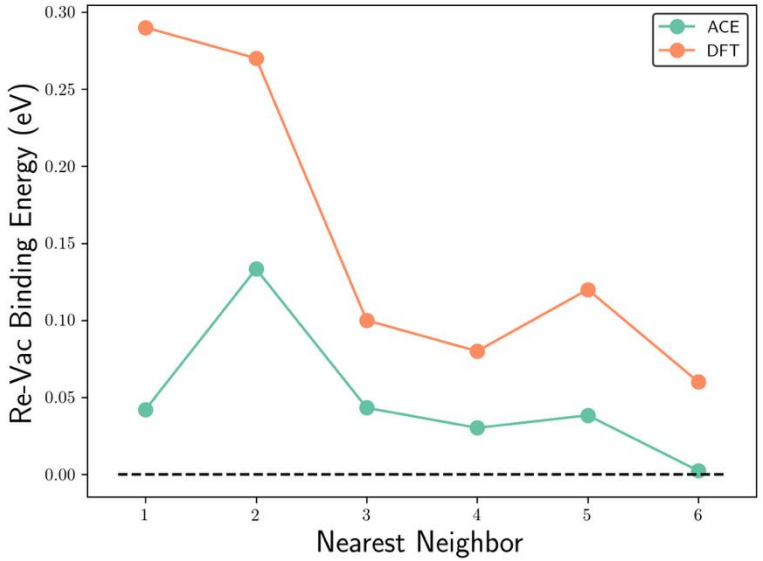

Developing Advanced Tungsten Materials

- Tungsten is currently a candidate material but suffers from a high ductile-to-brittle transition temperature and low recrystallization temperature
- Divertor material needs to balance a variety of properties

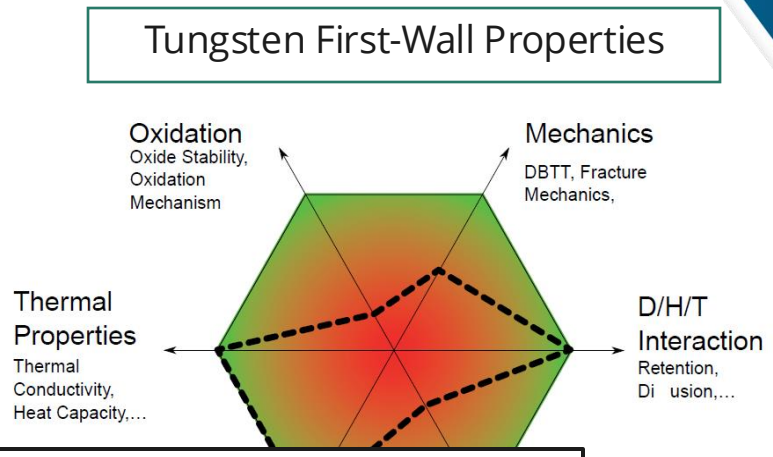

How do we optimize alloy composition when the parameter space is vast?

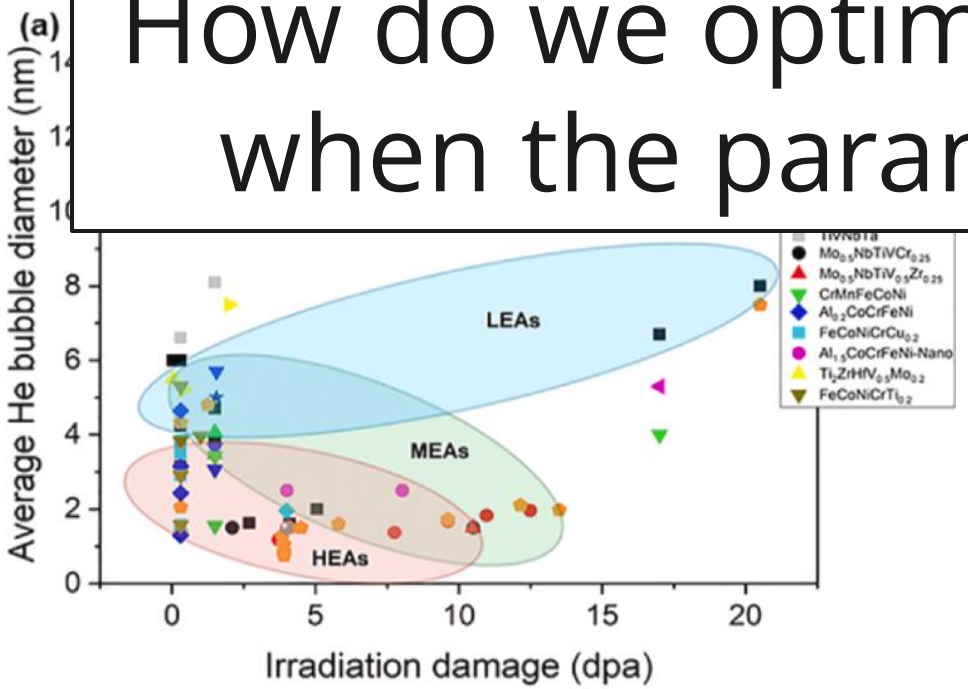

- Alloying tungsten with other elements has shown to increase strength properties but dependence on radiation tolerance is unknown

Z. Cheng , et al. Journal of Alloys and Compounds 930 (2023) 166768

Molecular Dynamics Can Quickly Sample Compositional Space

Compositional Analysis - MoNbTaTi

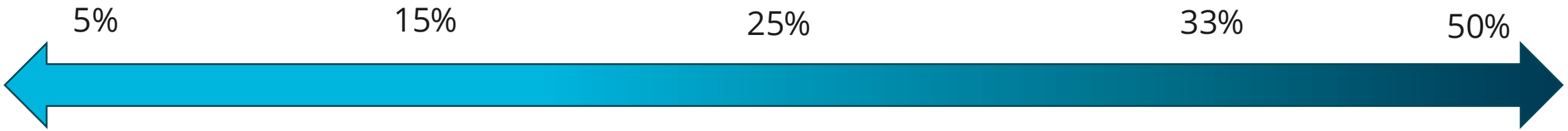

17 Total Compositions Analyzed

Simulations

- He implantation
  - 100 eV He implantation
  - 1000 K
  - (100) surface
  - 15 ns of simulation time
- Molecular statics
  - He formation energies
  - He migration barriers

Analysis

- Helium bubble damage and He energetics

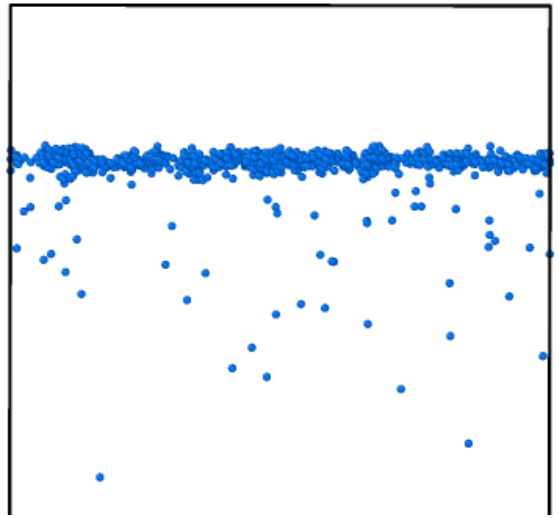

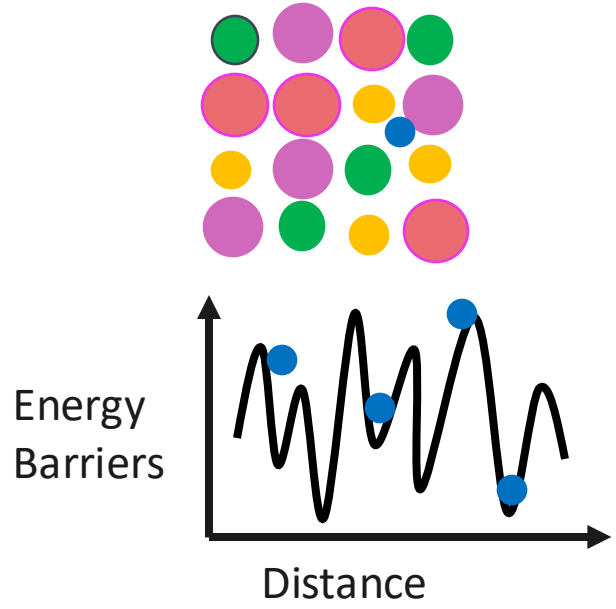

M.J. McCarthy, et al. J. Appl. Phys. 137, 175108 (2025)

Helium Cluster Size Increases with Atomic Volume per Composition

He Clustering at 15 ns

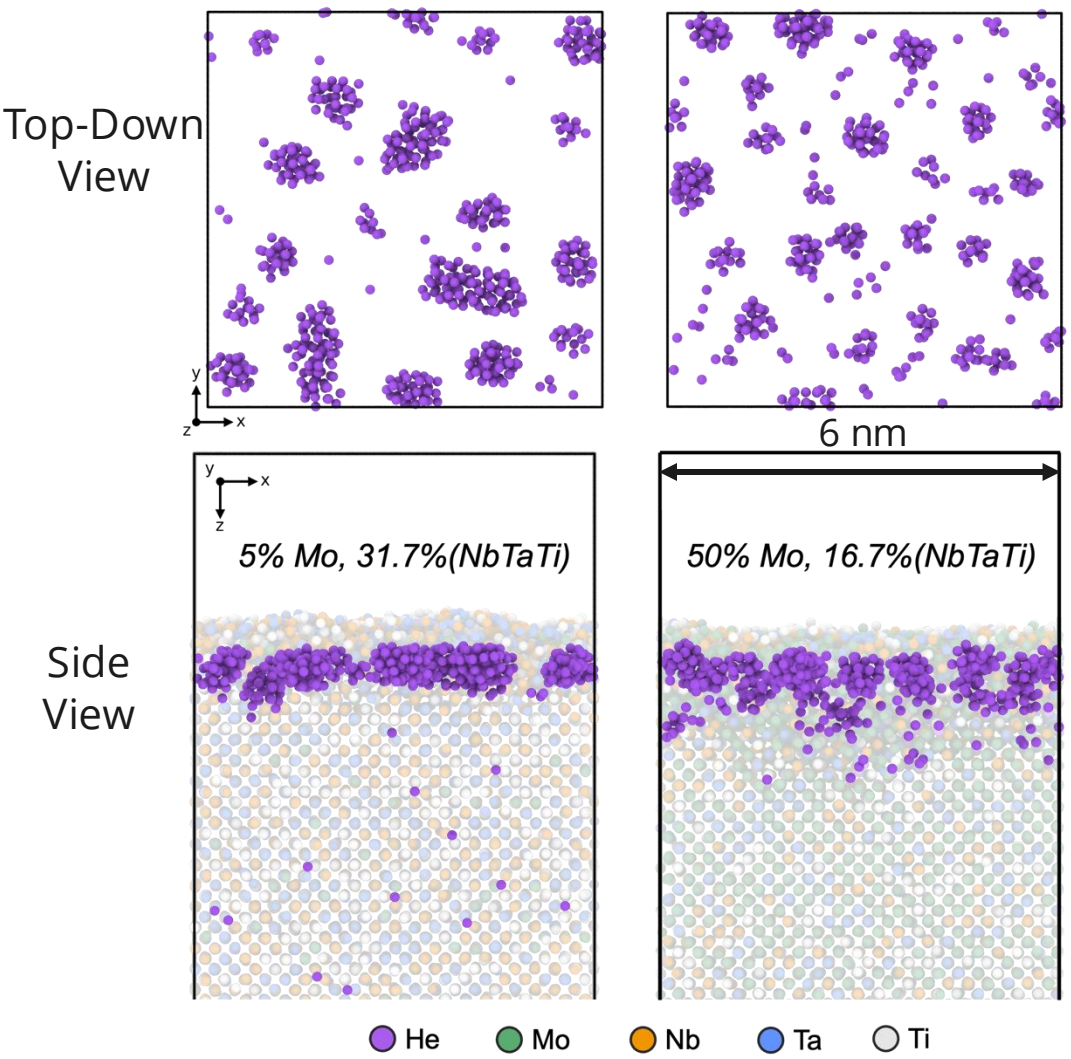

Cluster Size Increases with Increasing Atomic Volume
He/V Decreases with Increasing Atomic Volume

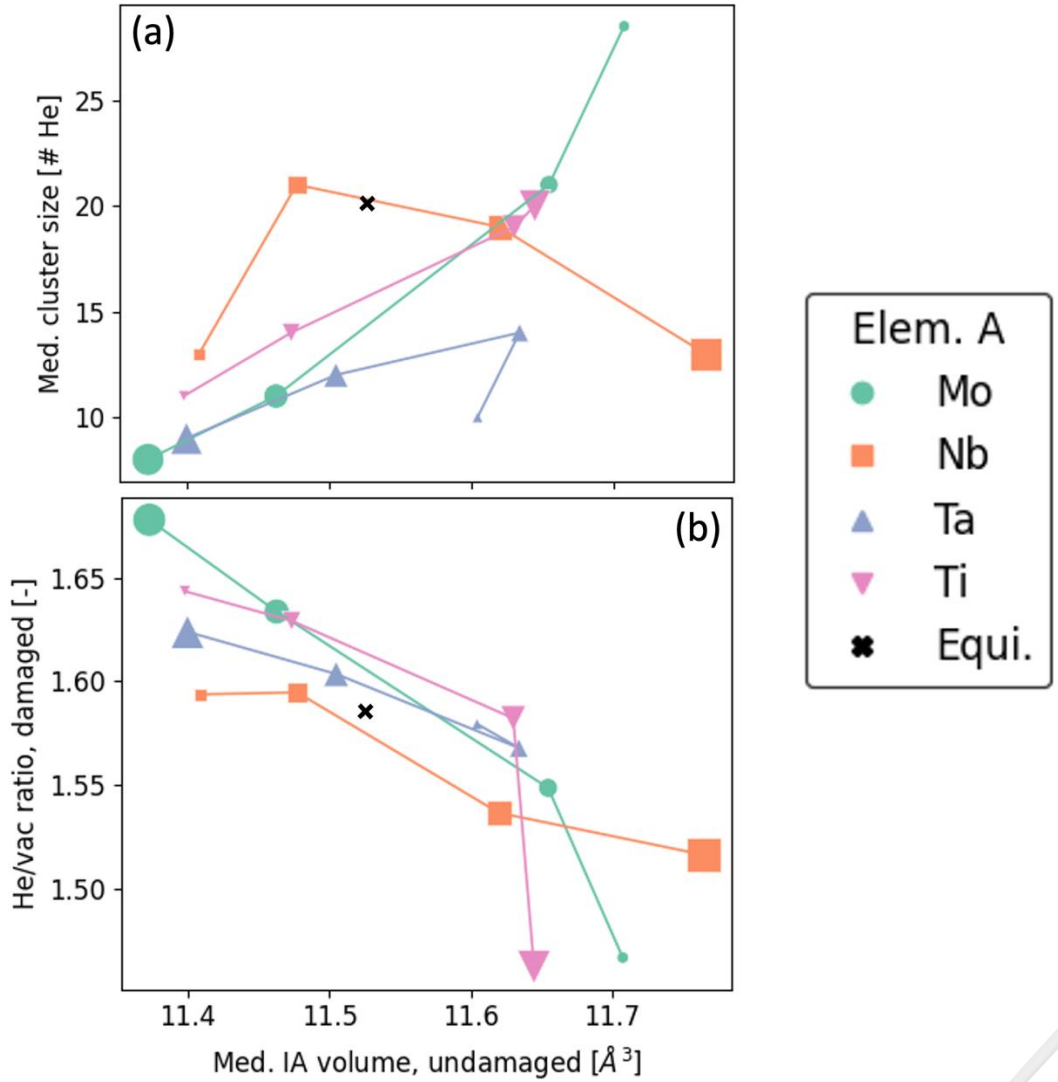

M.J. McCarthy, et al. J. Appl. Phys. 137, 175108 (2025)

Lower Atomic Volume Results in Increased Migration Barriers Which Reduces Cluster Size

Purple: Helium

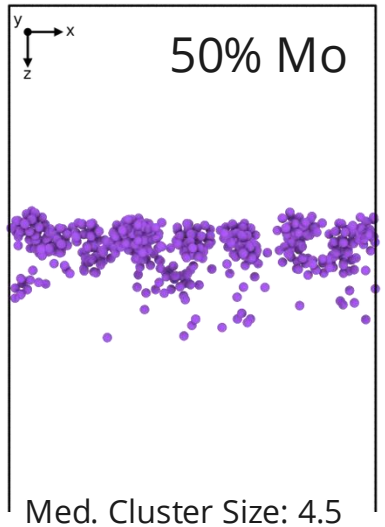

Med. Cluster Size: 4.5

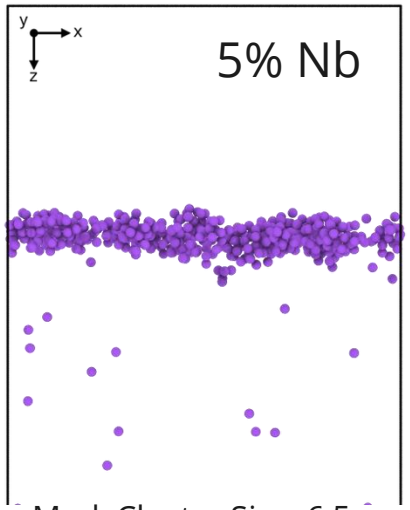

Med. Cluster Size: 6.5

Increasing atomic volume decreases the migration barrier

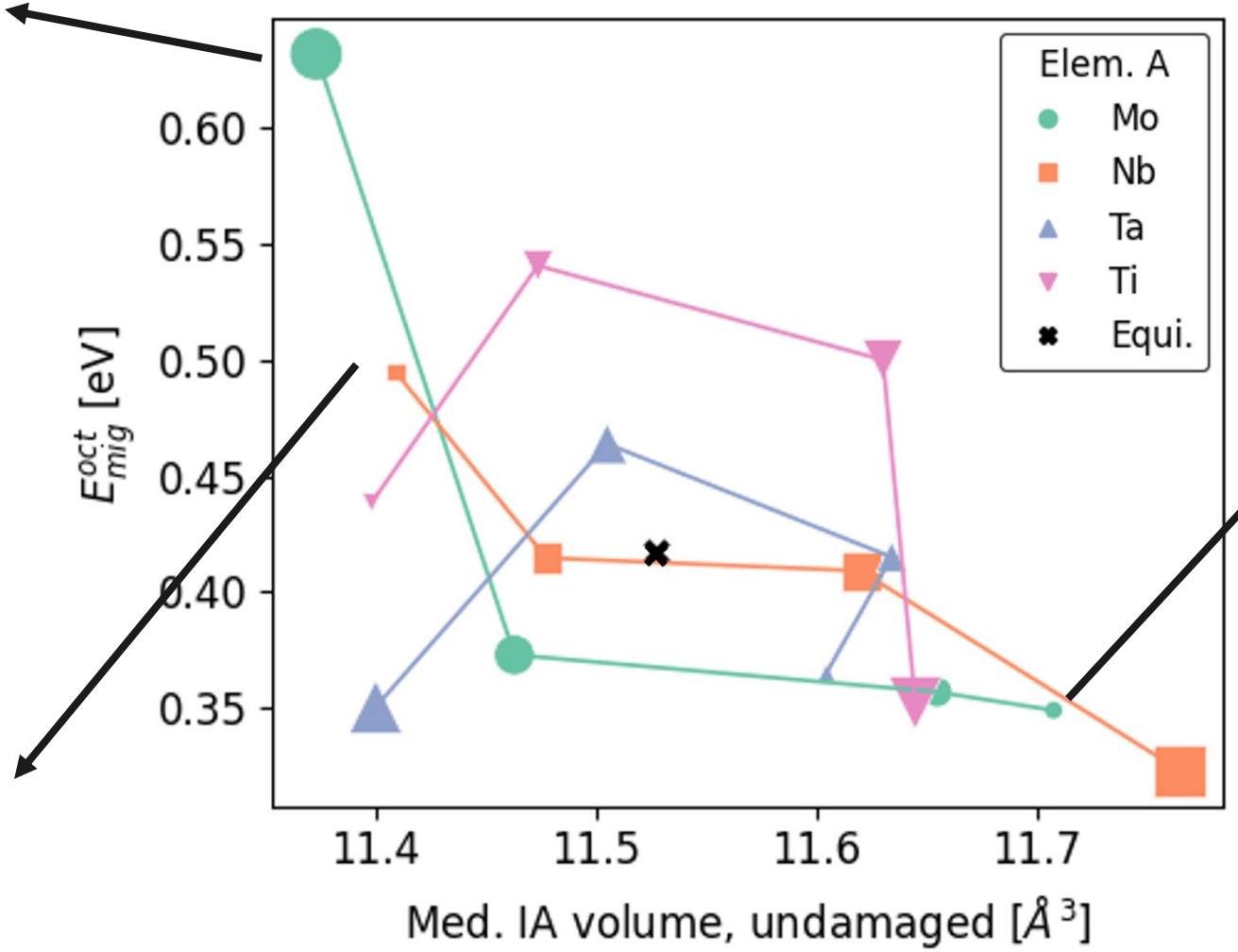

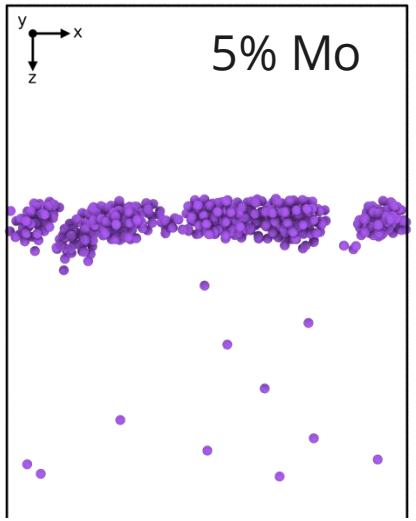

Med. Cluster Size: 14.5

M.J. McCarthy, et al. J. Appl. Phys. 137, 175108 (2025)

Testing Of Alloys Under Fusion Relevant Helium Plasmas

- Samples prepared using directed energy deposition
  - NbTa, NbTaMo, NbTaTi, NbTaMoTi
  - Testing of initial alloys from MD study
- Helium exposures performed at PISCES-RF linear plasma device at UCSD
  - 40 eV He flux of $7x10^{22}$ $m^{-2}s^{-1}$
  - Accumulated ion fluence of $2x10^{26}$ m^{-2} at 1000 K
  - Optical emission spectroscopy performed in-situ
- Post characterization performed at UNM:
  - SEM, FIB, SEM-EDS, SEM-EBSD, XPS

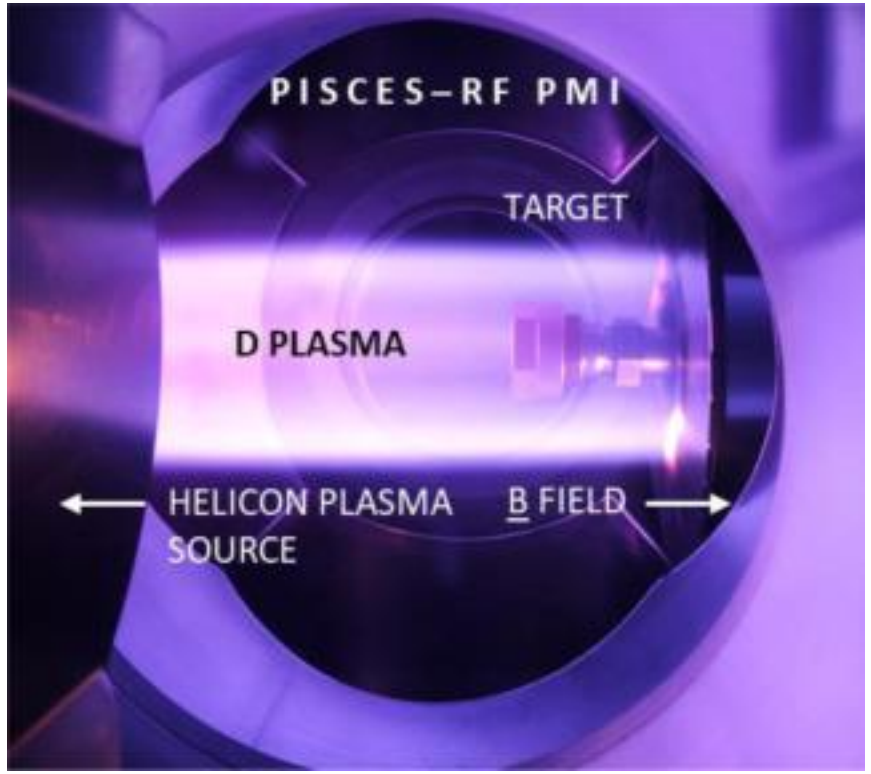

M. Baldwin, et al. Nuclear Materials and Energy 39 (2024) 101626

Local Composition Impacts Nanotendril Features

Nanostructuring Depends on Local Composition

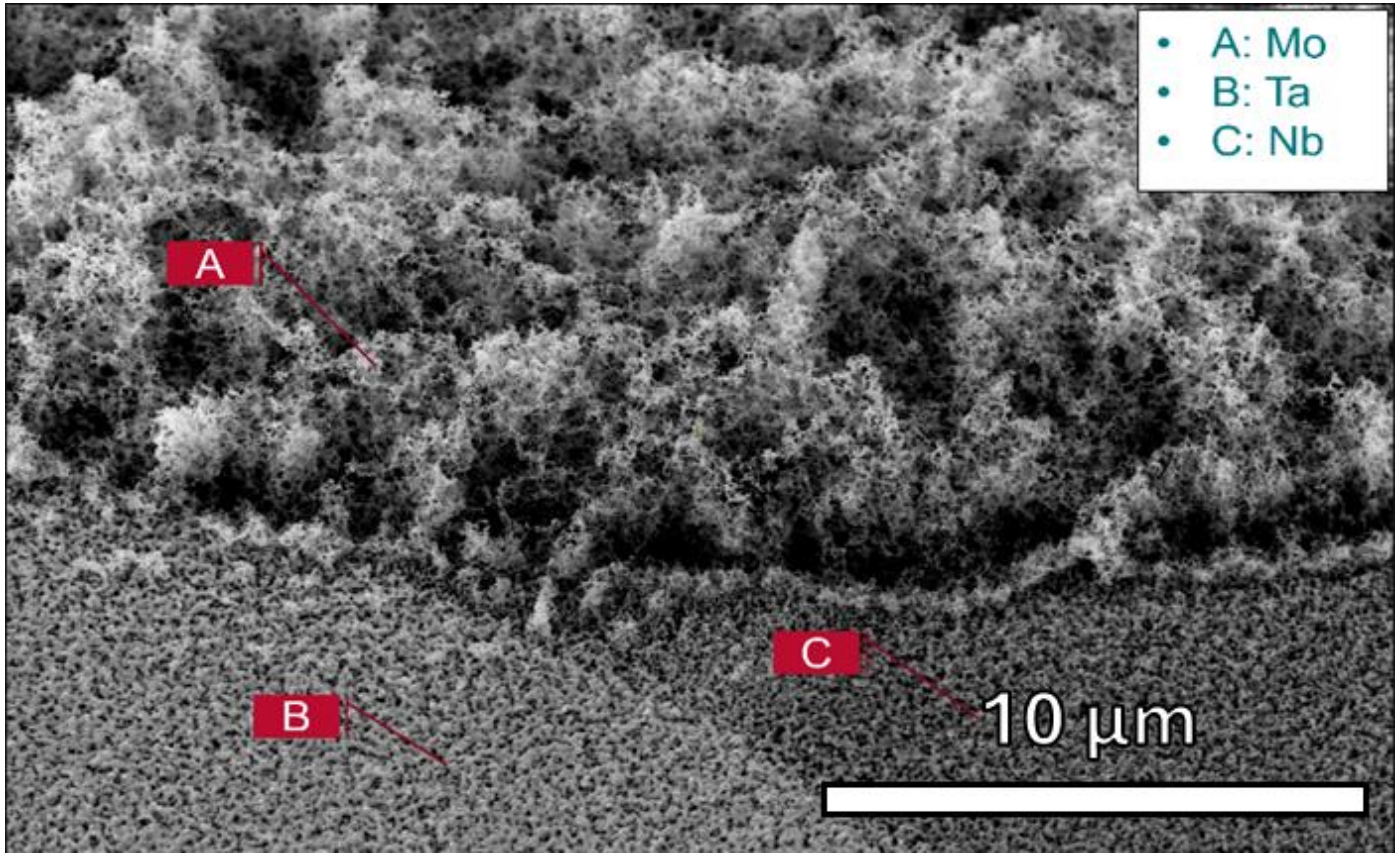

S. Evans, et al. Nucl. Mater. Energy (2025) Accepted

Local Composition Evolves Over Time Resulting In Enrichment/Depletion Of Different Elements In The Tendril And Bulk Regions

TaNbMo

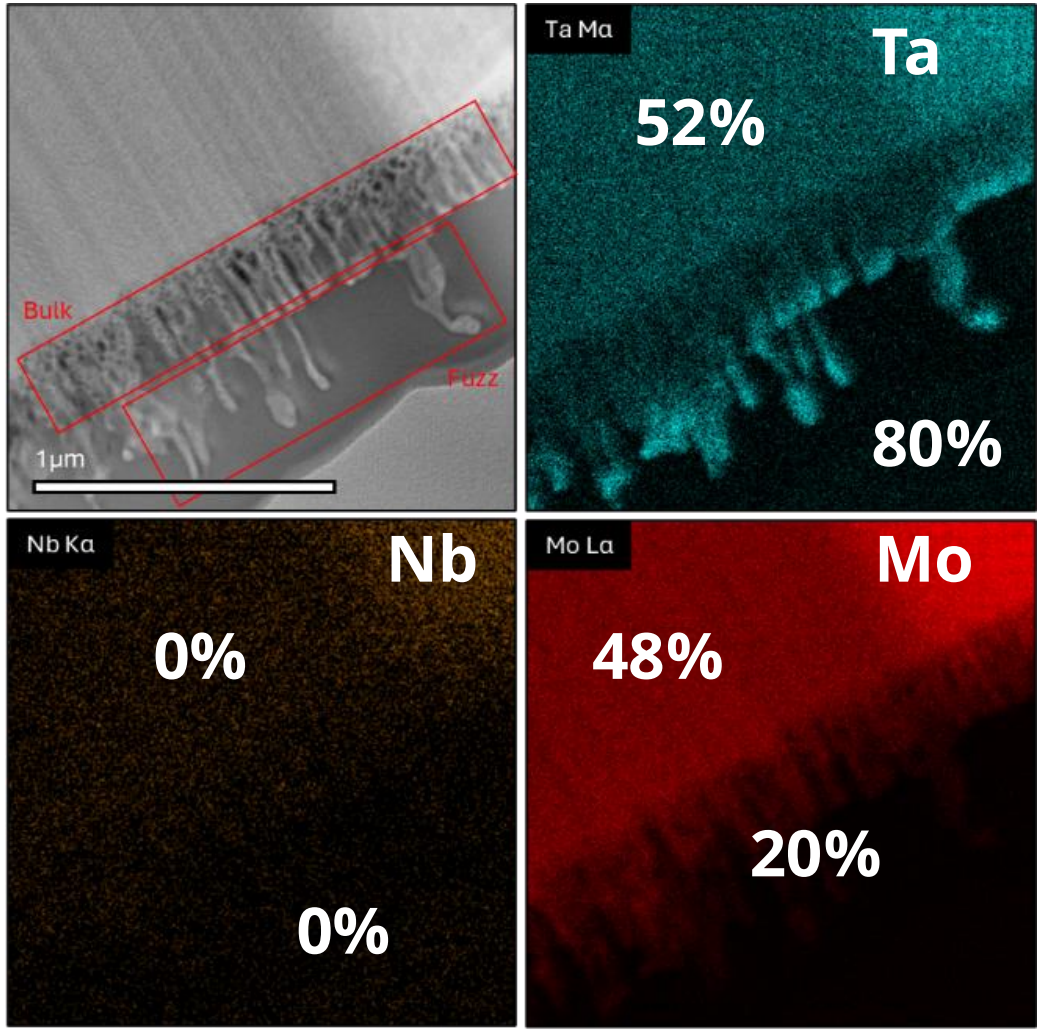

TaNbMoTi

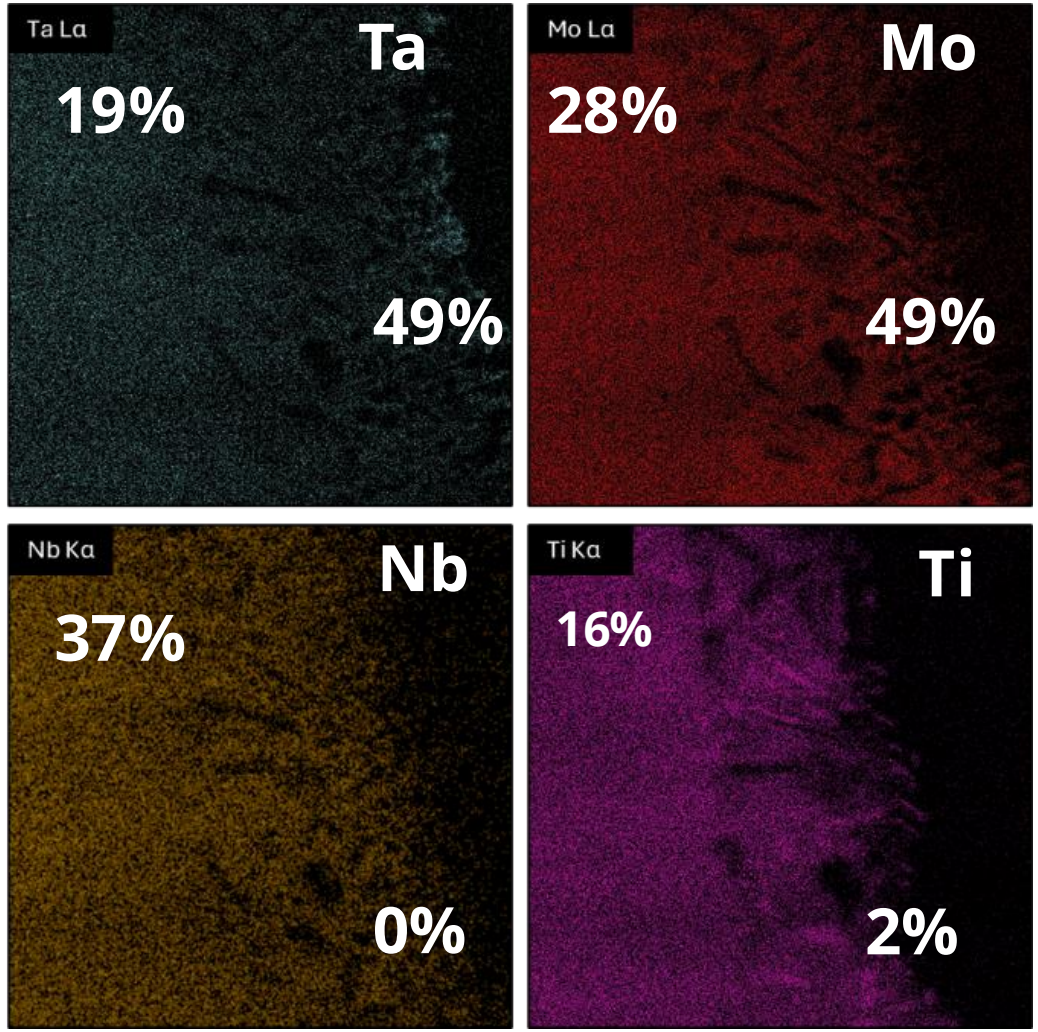

S. Evans, et al. Nucl. Mater. Energy (2025) Accepted

Lower Migration Barriers Result in Larger Bubble Size

He Implantations Under PISCES-RF conditions

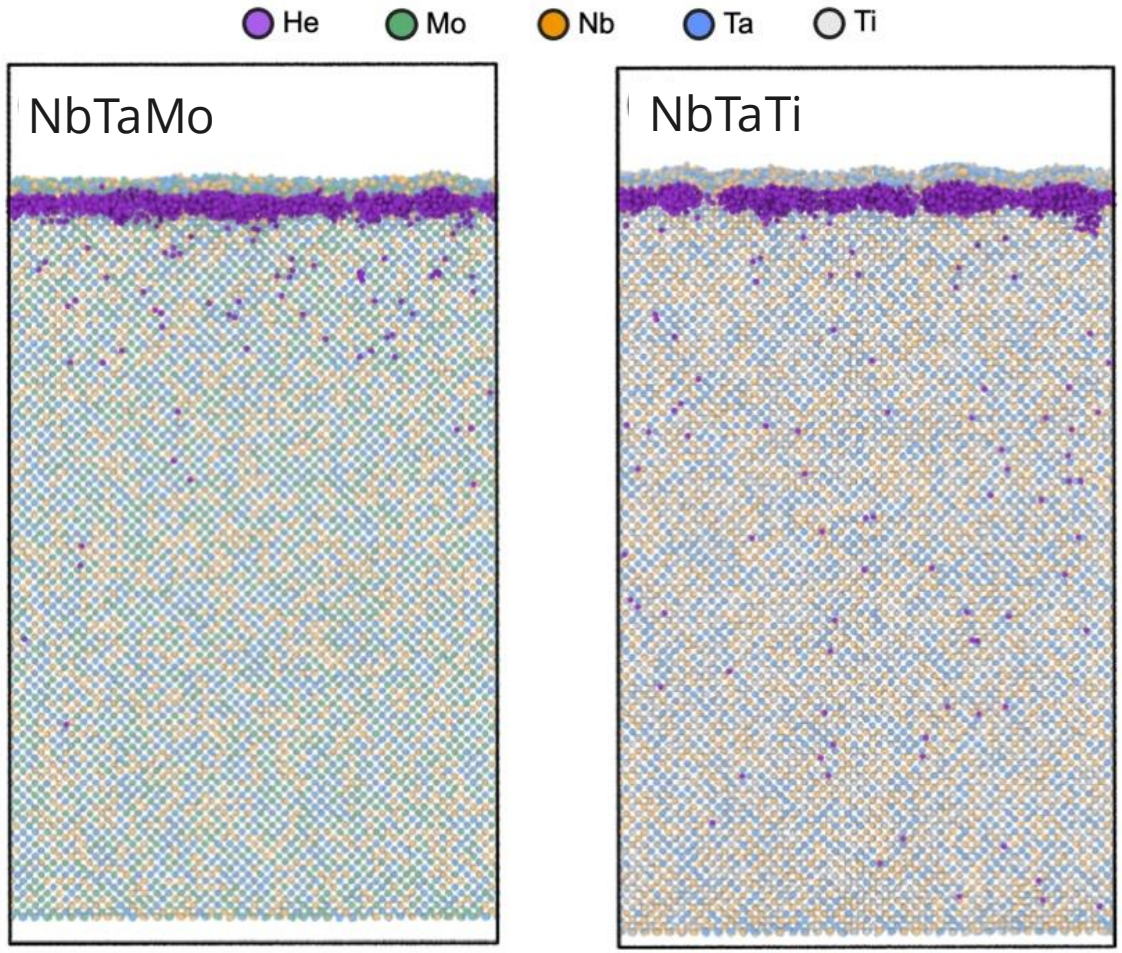

Bubble Sizes:
Experimental: 2.26 nm^3
MD: 4 He

Bubble Sizes:
Experimental: 5.87 nm^3
MD: 8 He

MD Migration Barriers vs. Experimental Bubble Size

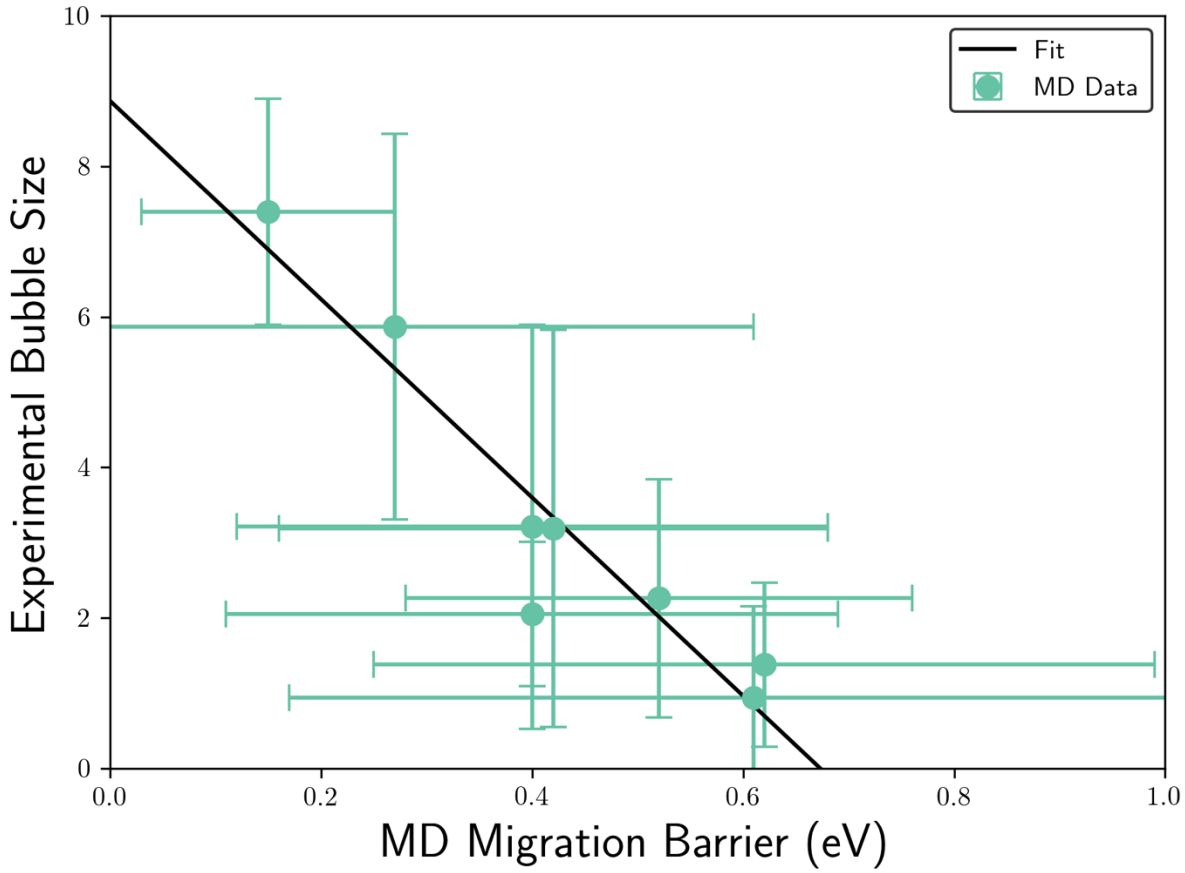

Summary and Future Work

Summary

- Designing plasm—facing components is challenging and requires information at the atomistic scale
- ML-IAPs like ACE can improve accuracy of chemically complex IAPs used for modeling extreme conditions
- We have developed multiple first wall ML-IAPS that incorporate transmutation products and multi-component potentials that reproduce experimental results

Future Work

- Further refinement of ML-IAPs
- Atomistic modeling of PKA damage with transmutation products
- Incorporation of H/He in ML-IAPs

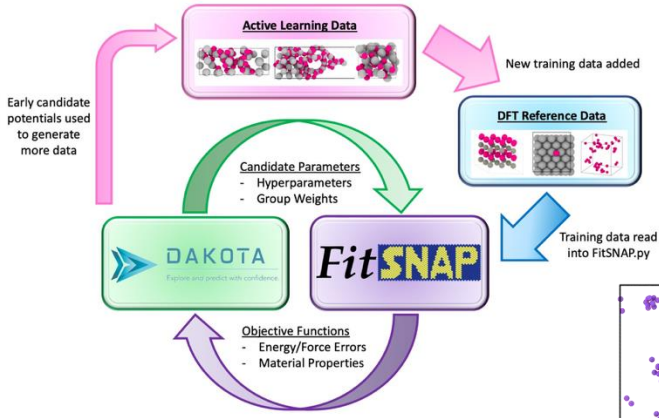

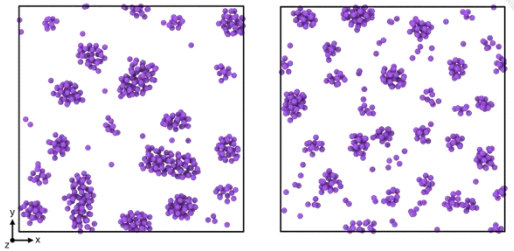

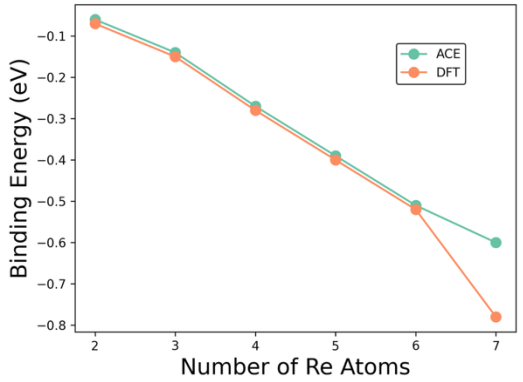

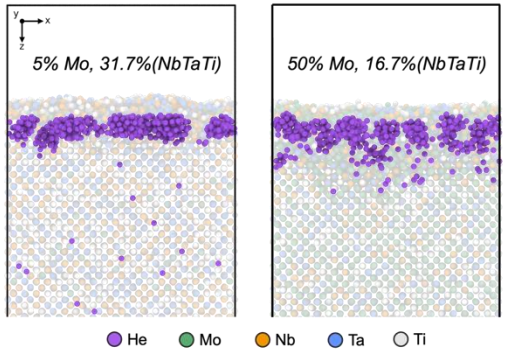

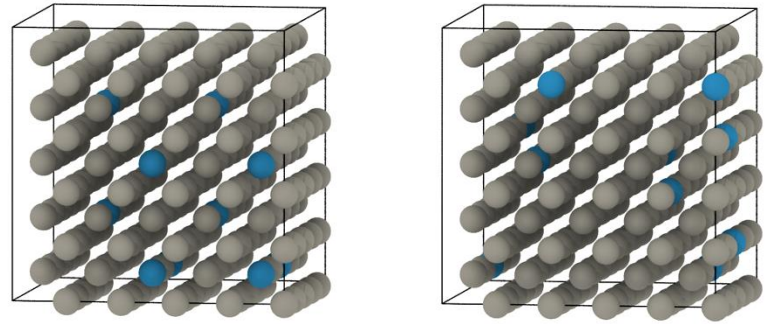

Contact:
mcusent@sandia.gov

Office of Science

Emission Spectroscopy Indicates Ti and Nb Preferentially Sputter

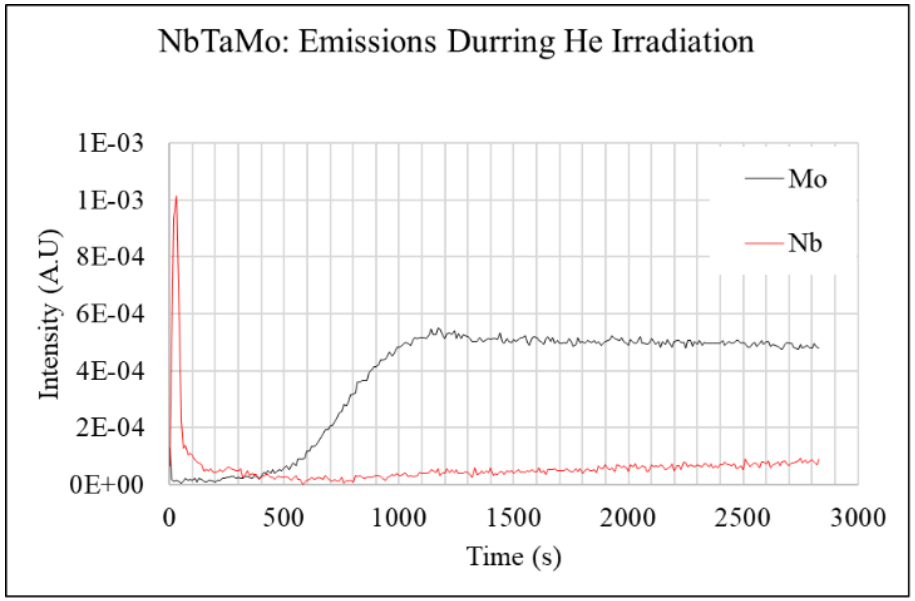

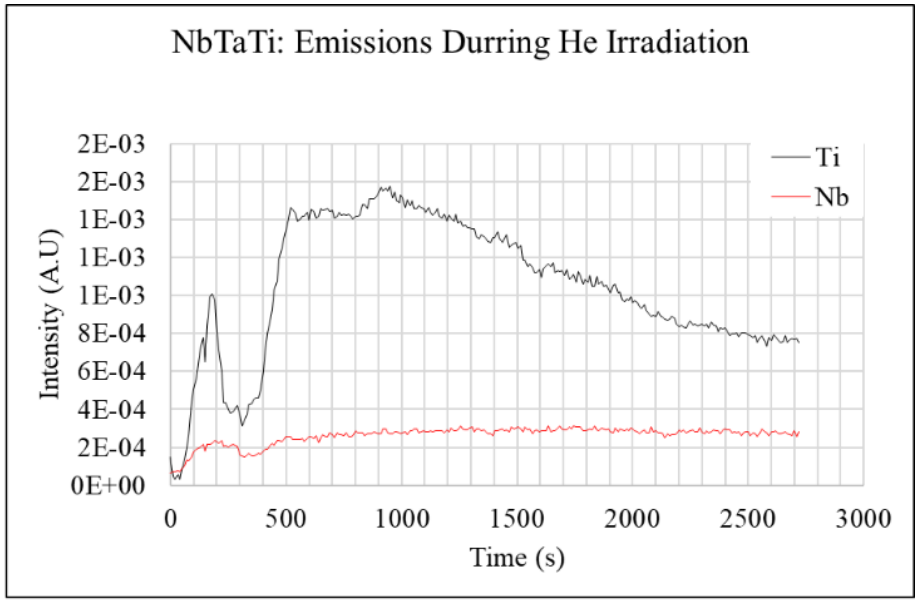

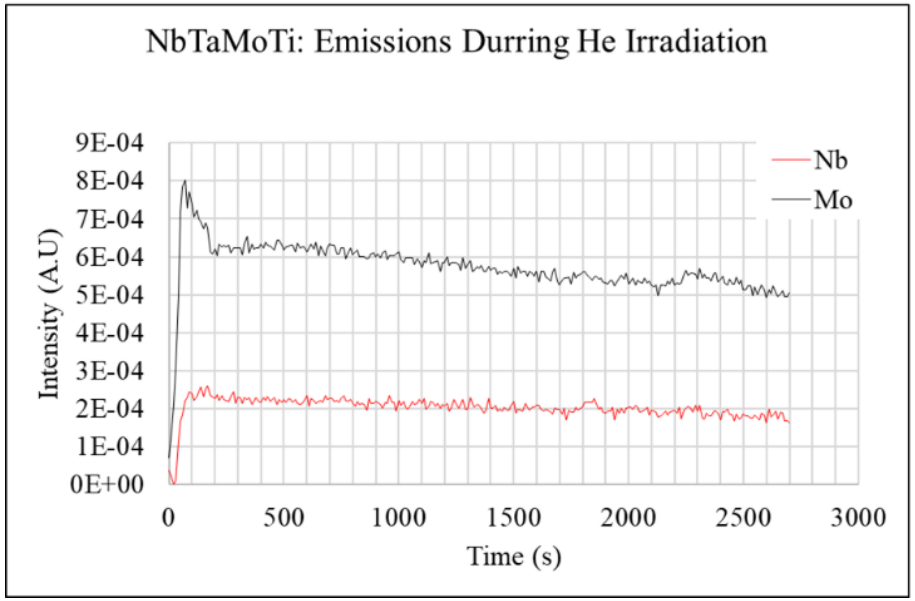

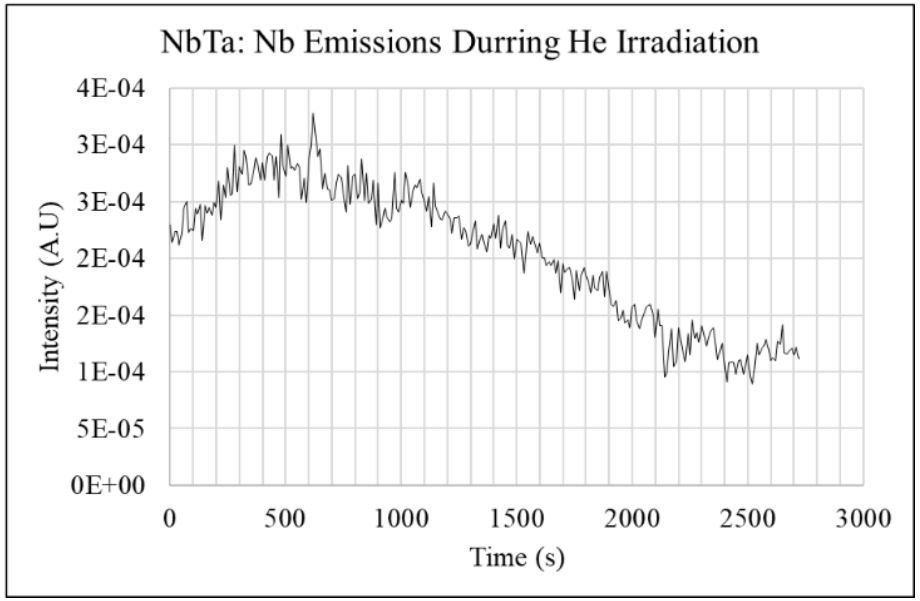

Lack of Ti and Nb in the tendrils is linked to sputtering of these elements as indicated by the spectroscopy data

Ti Is Less Strongly Bound to the Surface

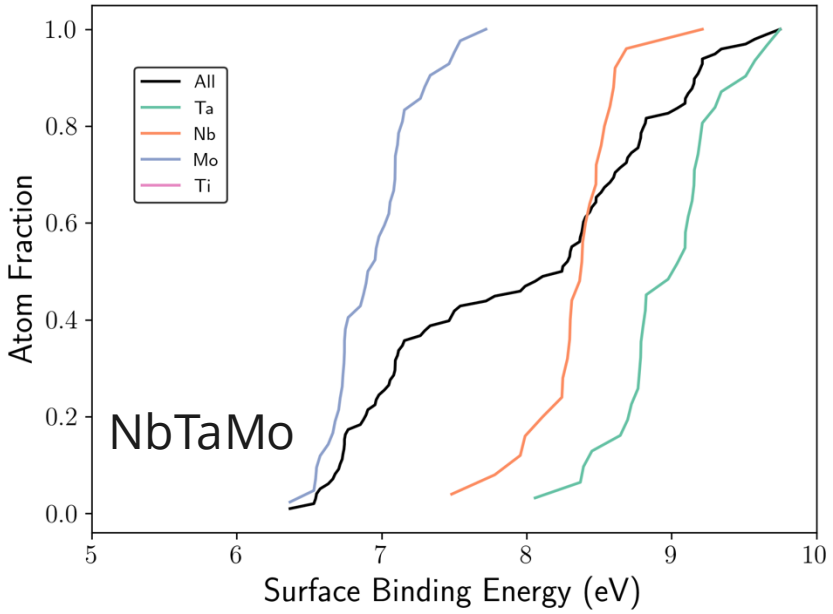

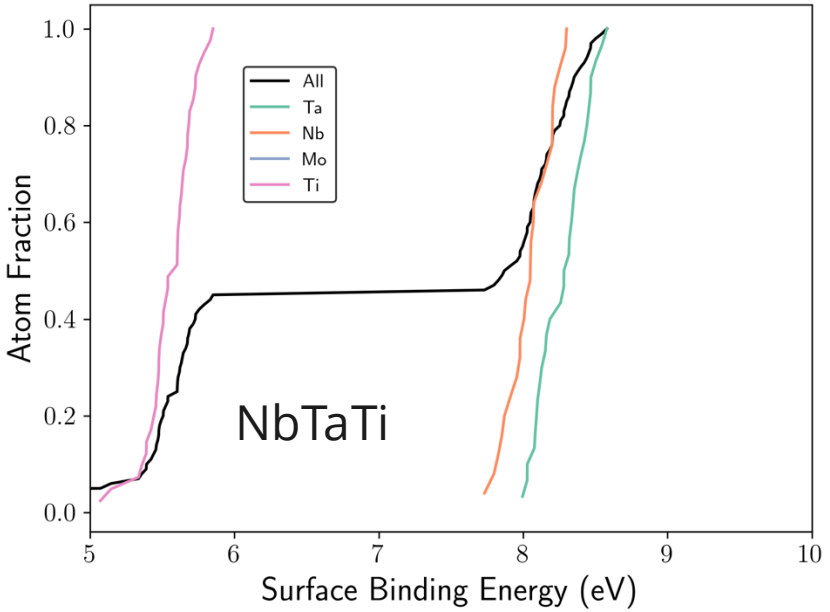

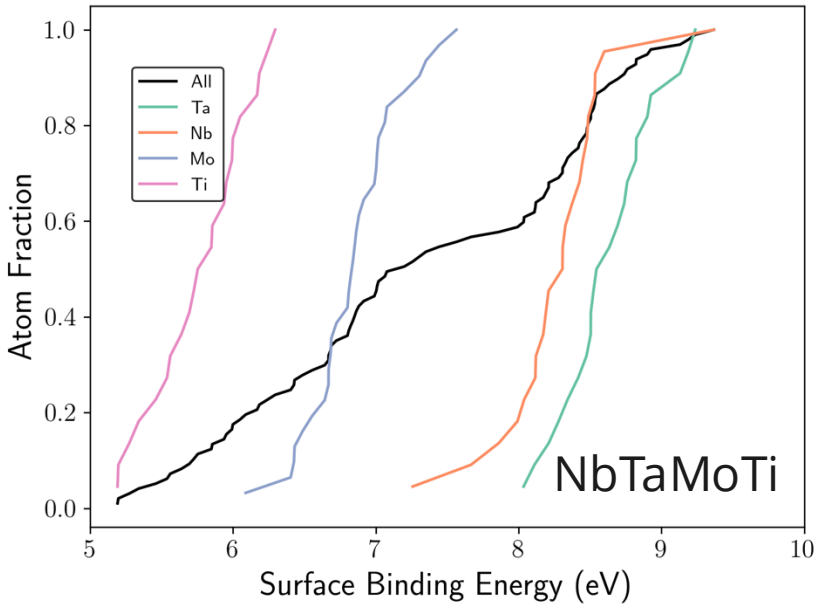

Ti has lowest surface binding energy resulting in increased sputtering

NbTaMo would likely have lowest sputtering due to highest average surface binding energy

Surface Binding Energy

Composition	Nb	Ta	Ti	Mo	Average
NbTaMo	8.28	9.04	-	6.93	8.25
NbTaTi	8.05	8.30	5.60	-	7.89
NbTaMoTi	8.31	8.59	5.80	6.84	7.20